

## Original Article

# Arsenic trioxide suppresses lung adenocarcinoma stem cell stemness by inhibiting m6A modification to promote ferroptosis

Wen Jin<sup>1\*</sup>, Yu Sun<sup>1\*</sup>, Jiaqi Wang<sup>2\*</sup>, Yan Wang<sup>1</sup>, Dan Chen<sup>2</sup>, Ming Fang<sup>1</sup>, Jie He<sup>1</sup>, Linsheng Zhong<sup>1</sup>, Hao Ren<sup>1</sup>, Yuanmei Zhang<sup>3</sup>, Hao Yin<sup>1</sup>, Shijia Wu<sup>1</sup>, Ruqin Chen<sup>4</sup>, Wen Yan<sup>2</sup>

<sup>1</sup>Department of Cardiac Intensive Care Unit, The Cardiovascular Hospital, The Second People's Hospital of Guangdong Province, Guangzhou 510310, Guangdong, China; <sup>2</sup>Department of Oncology, The Second People's Hospital of Guangdong Province, Guangzhou 510310, Guangdong, China; <sup>3</sup>Department of Ultrasound, The First Affiliate Hospital of Guangzhou Medical University, Guangzhou 510120, Guangdong, China; <sup>4</sup>Department of Traditional Chinese Medicine, The Second People's Hospital of Guangdong Province, Guangzhou 510310, Guangdong, China. \*Equal contributors.

Received March 6, 2023; Accepted January 22, 2024; Epub February 15, 2024; Published February 28, 2024

**Abstract:** Arsenic trioxide (ATO) is well known for its inhibitory effects on cancer progression, including lung adenocarcinoma (LUAD), but the molecular mechanism remains elusive. This study aimed to investigate the roles of ATO in regulating LUAD stem cells (LASCs) and the underlying mechanisms. To induce LASCs, cells cultured in an F12 medium, containing B27, epidermal growth factor, and basic fibroblast growth factor, induced LASCs. LASCs stemness was assessed through tumor sphere formation assay, and percentages of CD133+ cells were detected by flow cytometry. The Cell Counting Kit-8 method was used to assess LASCs viability, while reactive oxygen species (ROS) and iron ion levels were quantitated by fluorescence microscopy and spectrophotometry, respectively, and total m6A levels were measured by dot blot. Additionally, LASCs mitochondrial alterations were analyzed via transmission electron microscopy. Finally, the tumorigenicity of LASCs was assessed using a cancer cell line-based xenograft model. Tumor sphere formation and CD133 expression were used to validate the successful induction of LASCs from A549 and NCI-H1975 cells. ATO significantly inhibited proliferation, reduced ZC3H13 expression and total m6A modification levels, and increased ROS and iron ion content, but repressed sphere formation and CD133 expression in LASCs. ZC3H13 overexpression or ferrostatin-1 treatment abrogated LASCs stemness inhibition caused by ATO treatment, and interference with ZC3H13 inhibited LASCs stemness. Furthermore, the promotion of LASCs ferroptosis by ATO was effectively mitigated by ZC3H13 overexpression, while interference with ZC3H13 further promoted ferroptosis. Moreover, si-ZC3H13 promoted ferroptosis and impaired stemness in LASCs, which ferrostatin-1 abrogated. Finally, ZC3H13 overexpression alleviated the inhibitory effects of ATO on LASCs tumorigenicity. Taken together, ATO treatment substantially impaired the stemness of LUAD stem cells by promoting the ferroptosis program, which was mediated by its ZC3H13 gene expression inhibition to suppress m6A medication.

**Keywords:** Arsenic trioxide, lung adenocarcinoma, cancer stem cells, ferroptosis, ZC3H13, m6A

## Introduction

Lung adenocarcinoma (LUAD) is the most prevalent histological subtype of lung cancer, which is a non-small-cell lung cancer (NSCLC) subtype and accounts for nearly 40% of all lung cancer cases [1]. LUAD is usually derived from the abnormal transformation of alveolar epithelial type II cells that secrete mucus [1] and is well known for its 5-year mortality of 60%-99% [2, 3]. The high global incidence of LUAD is

closely associated with various risk factors such as cigarette smoking, carcinogen exposure in work conditions, and environmental pollution [3]. Recent progress during the past decades has demonstrated that mutations in a set of driver genes, such as genetic epidermal growth factor receptor, Kirsten rat sarcoma viral oncogene, and v-Raf murine sarcoma viral oncogene homolog B (BRAF), greatly facilitated LUAD initiation and progression [3-5]. The elucidation of genetic mutations driving LUAD devel-

opment guided the recent application of multiple targeted therapies such as erlotinib and gefitinib [1]. However, the incidence and mortality of LUAD remain at high levels, which necessitate the development of new therapeutic reagents and a full understanding of molecular pharmaceutical mechanisms.

Arsenic trioxide ( $\text{As}_2\text{O}_3$  [ATO]) is a major type of toxic arsenic that has been used in ancient Chinese medicine for treating multiple severe human disorders such as rheumatic diseases, syphilis, and psoriasis. ATO was recently discovered as a potent anticancer drug for acute promyelocytic leukemia and several solid cancer types with low toxicity [6]. Additionally, the effective anticancer roles of ATO have been recently mediated by its regulation of various biological processes such as cell apoptosis, oxidative stress, angiogenesis, cell cycle arrest, and cancer stem cell activities [6, 7]. Importantly, a potent therapeutic reagent for lung cancers has characterized ATO, but the responses of different lung cancer subtypes to ATO significantly vary [7]. In particular, early investigation revealed that ATO could repress the growth of both NSCLC and small cell lung cancer by inhibiting angiogenesis via modulating the vascular endothelial growth factor and Dll4-Notch signaling cascades [8]. The inhibitory effects of ATO on LUAD are mediated by multiple mechanisms, including suppression of E2F1 and thymidylate synthase [9, 10]. Furthermore, ATO inhibited the viability of cancer stem-like cells (CSLC) in lung cancer through Gli1 suppression, which is a major transcription factor in the Hedgehog pathway [11]. However, the effects of ATO on LUAD stem cells (LASCs) and the underlying mechanisms remain unclear.

Ferroptosis is a newly identified form of programmed cell death, which is generally induced by iron accumulation and phospholipid peroxidation and widely exists in various species, including mammals, higher plants, fungi, and protozoa [12, 13]. Recent research has revealed that ferroptosis integrated extracellular and intracellular signals, such as heat and radiation exposure, redox hemostasis, selenium metabolism, and multiple cellular signaling pathways [12]. Ferroptosis initiation and progression are mediated and regulated by interactions between many molecular machinery and signaling components [14]. Among them,

glutathione peroxidase 4 (GPX4) is a phospholipid hydroperoxidase responsible for reducing phospholipid and cholesterol hydroperoxide, which serves as the key inhibitor of phospholipid peroxidation, and GPX4 inhibition is a key downstream event during ferroptosis [12, 14]. Moreover, ferroptosis plays an essential role in various physiological and pathological processes, including tissue damage, inflammation, immune surveillance, and tumor development suppression [12, 15]. Therefore, ferroptosis is prevalently evaded during lung cancer progression [16, 17], and ferroptosis induction has been shown to mediate NSCLC inhibition by artemisinin derivatives [18]. However, little is known about the roles of ferroptosis in LUAD stem cells and its suppression by ATO. Moreover, N6-methyladenosine (m6A) modification catalyzed by methyltransferase-like protein 3 (METTL3) could initiate ferroptosis during LUAD development [19], but whether or not ATO regulates m6A modification to inhibit LUAD remains unclear.

This study aimed to explore the possible roles of ATO in modulating the ferroptosis program to regulate LASCs activity, as well as the implication of m6A modification regulation in such processes. These investigations provide a new perspective on the pharmaceutical mechanisms underlying LUAD inhibition by ATO, which may provide new clues for developing novel therapeutic reagents for lung cancer treatment.

### Material and methods

#### *Cell culture and treatment*

The LUAD cell lines A549 (#CC0202) and NCI-H1975 (#CC0206) were obtained from the CellCook Company (Guangzhou, China) and separately cultured in F-12K medium (#BL-311A; Biosharp, Hefei, China) and RPMI 1640 (#CM2017, CellCook), supplemented with 10% fetal bovine serum (FBS, #A3160802; Gibico), at 37°C in a humidified atmosphere with 5%  $\text{CO}_2$ . Short tandem repeat profiling was performed to validate LUAD cell line identity. The induction of A549 and NCI-H1975 cell development toward LASCs was performed as described below, which were cultured in a medium containing 0.625, 1.25, 2.5, 5, 10, 20, or 40 mM ATO (#H20080664; SL Pharm, Beijing, China) followed by normal culture for another 24 or 48 h.

# Arsenic trioxide promotes ferroptosis in lung adenocarcinoma stem cells

## *Stem cell induction and sphere formation*

LASCs were induced from A549 and NCI-H1975 cell lines by culturing with a medium containing B27, EGF, and basic fibroblast growth factor (bFGF). Briefly, cultured A549 and NCI-H1975 cells in the logarithmic growth phase were washed twice with PBS solution and treated with 1.0 ml of 0.25% trypsin solution for an appropriate time, followed by the addition of 10% FBS to terminate trypsin digestion. Cells were then collected by centrifugation at 800 rpm for 5 min, seeded in 6-well plates (30-50 cells/well), and cultured under 37°C and 5% CO<sub>2</sub> for approximately 6-8 days until cell clone formation in the 6-well plates. Single-cell clones from A549 and NCI-H1975 cells were then collected and digested with 0.25% trypsin solution again, which were collected by centrifugation at 800 rpm for 5 min, resuspended in F12 medium containing 2% B27, 20 ng/ml of EGF, and 20 ng/ml of bFGF, and planted in new 6-well plates (10<sup>3</sup> cells/well), followed by culture at 37°C for another week until suspended stem cell spheres in regular sizes and shapes were clear under microscopy.

## *Cell surface marker detection*

The expression of the cell surface biomarker protein CD133 in induced LASCs was assessed quantitatively by the percentages of CD133-positive cells using flow cytometry. In brief, approximately 10<sup>6</sup> LASCs were first blocked in 100 µl of blocking buffer (PBS solution containing 2% BSA and 1% FBS) for 15 min in darkness, which were then incubated in darkness with diluted antibodies, including CD133 APC Mab (#FAB11331A-100; R&D Systems) and APC Mouse IgG2a Isotype Control (#E-AB-F09802E; Elabscience Biotechnology) for 30 min at 4°C. Subsequently, these LASCs cells were washed twice with 3 ml of PBS solution, resuspended in 500 µl of PBS solution, and finally analyzed by ACEA NovoCyte flow cytometry.

## *Cell viability detection*

The viability of cultured LASCs was evaluated in this study using the Cell Counting Kit-8 (CCK-8) (#G4103; ServiceBio, Wuhan, China) following the manufacturer's instructions. Briefly, cultured LASCs in the logarithmic growth phase were first washed once with PBS solution,

digested with appropriate 0.25% trypsin solution, resuspended (3 × 10<sup>4</sup> cells/ml), seeded in 96-well plates (100 µl/well), and cultured at 37°C for 24 and 48 h, which were then mixed with 10 µl of CCK-8 solution followed by culturing at 37°C for another 2 h. Finally, the viability of cultured LASCs was determined by measuring the OD450 values on a microplate reader.

## *Quantitative reverse transcription PCR (RT-PCR)*

This study detected the relative mRNA levels of target genes by quantitative RT-PCR. Briefly, total RNA samples from cultured cancer stem cells or tumor tissues were prepared using Triquick Reagent (Trizol Substitute) (#R1100; Solarbio, Beijing, China) following the manufacturer's instructions. The cDNA samples were then synthesized from 2 µg of total RNA using the HiScript III RT SuperMix for qPCR (#R323-01; Vazyme, Nanjing, China) following the manufacturer's instructions. Subsequently, target gene expression was detected via real-time quantitative PCR using the ChamQ Universal SYBR qPCR Master Mix (#Q711-02; Vazyme, Nanjing, China) following the manufacturer's instructions. The relative expression levels were finally calculated using the standard 2<sup>-ΔΔCt</sup> method. **Table 1** lists the primers used for quantitative PCR assay in this study.

## *Western blot*

Total proteins were extracted from cultured LASCs or tumor tissues using RIPA lysis buffer (#P0013B; Shanghai, Beijing, China) following the manufacturer's instructions. The concentration of protein samples was determined using the BCA method using a protein quantitation kit (#BL521A; Biosharp, Hefei, China). Subsequently, an appropriate volume of protein samples was boiled at 98°C for 5 min, separated through SDS-PAGE, and blotted onto polyvinylidene fluoride membranes, which were then blocked with 5% lipid-free milk solution and incubated with the primary and secondary antibodies following standard procedures. Finally, protein expression was developed using enhanced chemiluminescent substrates (#BL-520A; Biosharp, Hefei, China). The primary antibodies used in this study are as follows: anti-METTL14 (#A8530; ABCLONAL), anti-METTL16 (#A15894; ABCLONAL), anti-Wilms' tumor 1-associating protein (WTAP) (#A14695; ABCL-

## Arsenic trioxide promotes ferroptosis in lung adenocarcinoma stem cells

**Table 1.** Information of primers used in quantitative PCR assay

Gene ID	Primer sequences (5' to 3')	Product length (bp)
METTL14-F	GGGGTTGGACCTTGAAGAG	156
METTL14-R	CCCATGAGGCAGTGTTCCTT	
METTL16-F	ACTTTTGCATGTGCAACCCTC	232
METTL16-R	GCCAGGCTGCATTTCTTTCC	
WTAP-F	ACCAACGAAGAACCTCTTCCC	204
WTAP-R	AGACTCCTGCTGTTGTTGCT	
ZC3H13-F	CCTGGGGCTGCACTCTTAA	150
ZC3H13-R	AAGTAAATGAACTACCTTTGGGT	
FTO-F	TTGCCCGAACATTACCTGCT	92
FTO-R	TGTGAGGTCAAACGGCAGAG	
ALKBH5-F	GCCGTCATCAACGACTACCA	208
ALKBH5-R	ATCCACTGAGCACAGTCACG	
GPX4-F	TGAAGATCCAACCAAGGGC	84
GPX4-R	AGCCGTTCTTGTGATGAGG	
GAPDH-F	GAGTCAACGGATTGGTCGT	185
GAPDH-R	GACAAGCTTCCCCTTCTCAG	

ONAL), anti-ZC3H13 (#TD4623; ABMART), anti-FTO (#A1438; ABCLONAL), anti-ALKBH5 (#A11-684; ABCLONAL), and anti-GAPDH (#60004-1-Ig; proteintech).

### Dot blotting

The total levels of m6A in cultured LASCs and tumor tissues were quantitated by the dot blotting assay as follows. Briefly, total RNA samples were extracted from cancer stem cells or tumor tissues from naked mice as described above, which were then diluted into a concentration gradient, denatured at 95°C followed by immediate chilling, and transferred onto a nylon membrane. Subsequently, these membranes were subjected to automatic cross-linking under ultraviolet radiation, removal of unbound RNA samples, incubation with diluted antibodies recognizing N6-methyladenosine (m6A) (#ab208577; ABCAM) at 4°C under gentle shaking, three washes with washing buffer for 5 min each, followed by incubation with mouse anti-rabbit IgG-HRP antibodies (#BL003A; Biosharp, Hefei, China), and wash with washing buffer again. Finally, nylon membranes were developed using Western Blotting Substrate (#BL520A; Biosharp, Hefei, China).

### Reactive oxygen species (ROS) quantitation

The ROS levels in cancer stem cells and tumor tissue slides were measured using the ROS

Detection Kit (#BL714A; Biosharp, Hefei, China) following the manufacturer's instructions. Briefly, LASCs or tumor tissue slides were incubated in darkness with appropriate volumes of H2DCFDA working solution for 30 min at 37°C, were then washed twice with serum-free culture medium, and finally observed under a fluorescence microscope with a fluorescein isothiocyanate optical filter. At least three biological replicates were used for statistical analysis.

### Iron ion detection

The total iron ion (Fe) contents in LASCs or tumor tissues were quantitatively detected using the Tissue Iron Assay Kit (#A039-2-1; Nanjing Jiancheng Bioengineering Institute, Nanjing, China) following the manufacturer's protocol. Briefly, cancer stem cells or tumor tissues were collected and homogenized on ice, which were centrifuged at 2000 rpm for 15 min, and the supernatant was collected for quantitating protein concentration as described above. Subsequently, the supernatants were mixed with 1.5 ml of dipyrindine solution, boiled at 98°C for 5 min, cooled to room temperature, and centrifuged at 3500 rpm for 10 min. The OD520 values were detected on a spectrophotometer. Three biological repeats were performed for statistical analysis of iron ion levels.

### Transmission electron microscopy

The mitochondrial morphology in cultured LASCs was evaluated using transmission electron microscopy. Briefly, the cultured LASCs after specified treatments were collected and fixed in 2.5% glutaraldehyde for 3 h at 4°C, washed 6 times with 0.1 M of PBS solution at 4°C for 30 min, incubated with 1% osmic acid (#18456; TED PELLA, USA) for 1 h at 4°C, washed three times with 0.1 M of PBS solution for 5 min each, dehydrated using a graded series of ethanol and acetone solutions, and immersed in resin for 4 h. Subsequently, ultra-thin sections were made from fixed cell masses, which were finally observed using transmission electron microscopy (Japan Electron Optics Laboratory Co., Ltd., JEM-1400 PLUS). At least three repeats of transmission electron

## Arsenic trioxide promotes ferroptosis in lung adenocarcinoma stem cells

microscopy were performed to evaluate mitochondrial morphological alterations.

### *Cell transfections*

The coding sequences of the ZC3H13 gene were purified by PCR from cultured LASCs, which were then ligated with the pCDH-CMV-EF1A-EGFP-T2A-PURO plasmid (#P0268; MiaoLing-Bio, Wuhan, China) for the overexpression of the ZC3H13 gene. GeneCFPS Company (Wuxi, China) synthesized siRNA fragment 1 sequences targeting ZC3H13 (5'-CAGCAAUUUAGAAG-GUCACCAGAA-3'), siRNA fragment 2 sequences targeting ZC3H13 (5'-GGGAAUUAUGAAG-CUGGAACAAGA-3'), and the corresponding negative control (NC) sequences (5'-CAGATTAAGATTGGACCACAACGAA-3') to silence ZC3H13 expression in cultured LASCs. The above recombinant plasmid or siRNA sequences were transfected into LASCs cells using the Lip2000 Transfection Reagent (#BL623B; Biosharp, Hefei, China) following the manufacturer's instructions.

### *In vivo tumorigenicity*

The tumorigenicity of LASCs was evaluated using the cancer cell line-based xenograft (CDX) model. In brief, 18 BALB/c nude mice were randomly divided into three groups (6 mice per group), including the NC group, the ATO group, and the ZC3H13 + ATO group. Mice in the ATO group and the ZC3H13 + ATO group were intraperitoneally injected with 1  $\mu$ mol of ATO (#H20080664; SL Pharm, Beijing, China) every 3 days, which was done three times. Subsequently, nude mice were subcutaneously injected with  $3 \times 10^6$  LASCs or ZC3H13-overexpressing LASCs at the rear flank, followed by intraperitoneal injection of 1  $\mu$ mol of ATO every 3 days, which lasted for 4 weeks, until visible tumor tissues were formed in nude mice. Finally, the tumor tissues formed in nude mice were measured and collected for the following assays. The same treatments were administered to mice in the NC group, except that mice were injected with the same volume of normal saline before the injection of LASCs other than ATO.

### *Immunofluorescence*

The in-situ expression of CD133 antigen in tumor tissues was analyzed using the immuno-

fluorescence method. Briefly, tumor tissues derived from LASCs in nude mice were first immersed in sucrose solution and then in a 1:1 mixture of sucrose and tissue embedding medium (#G6059-110ML; ServiceBio, Wuhan, China) for 2 h at room temperature, followed by two further rounds of immersion at room temperature in tissue embedding medium for 4 h and 6 h, respectively. Tissue slides (10  $\mu$ m in thickness) were then made from the above tumor tissues, fixed with 4% PFA (in PBS) for 10 min at room temperature, washed twice with 0.1% Triton X-100 in PBS for 5 min, blocked with 3% blocking serum diluted in PBS for 1 h at room temperature, washed three times with PBS for 2 min, incubated with diluted primary antibodies (in 3% BSA solution) overnight at 4°C, washed again three times with PBS, and incubated with fluorescence-conjugated secondary antibody solution in darkness for 1 h at room temperature. Finally, tissue slides were counterstained with DAPI solution in darkness and were then mounted and analyzed under fluorescence microscopy.

### *Statistical analysis*

Quantitative data obtained from at least biological replicates are presented as mean  $\pm$  standard deviation and analyzed using Statistical Package for the Social Sciences version 20.0 software. Differences between groups were evaluated by Student's *t*-test or analysis of variance as appropriate, and a *P*-value of  $< 0.05$  indicated significant differences.

## Results

### *ATO inhibited proliferation and m6A modification in LASCs*

We first established a cellular LASCs model by inducing A549 cells and NCI-H1975 cells using a sphere formation medium (F12 containing B27, EGF, and bFGF) to investigate the cellular regulatory effects of ATO on LASCs, as introduced in the Materials and Methods section. We observed the significant tumor sphere formation from cultured A549 cells after treatment with sphere formation medium through the sphere formation assay for 1, 3, 5, and 7 days in a treatment time-dependent manner (**Figure 1A**), as well as that from cultured NCI-H1975 cells after treatment with sphere forma-

## Arsenic trioxide promotes ferroptosis in lung adenocarcinoma stem cells

tion medium for 1, 3, and 7 days in a treatment time-dependent manner ([Supplementary Figure 1A](#)). Our flow cytometry assay revealed that the percentages of stem cell marker gene CD133-positive cells in induced LASCs were significantly upregulated after inductive treatment for 7 days (**Figure 1B** and [Supplementary Figure 1B](#)). These results revealed that we successfully induced LASCs formation from A549 and NCI-H1975 cells, which were used for the following assays.

Subsequently, these induced LASCs were treated with 0, 0.625, 1.25, 2.5, 5, 10, 20, or 40 mM of ATO for 24 or 48 h, followed by the measurement of LASCs proliferation using the CCK-8 assay (**Figure 1C** and [Supplementary Figure 1C](#)). We revealed that ATO treatment induced significant inhibition of LASCs proliferation rates in a concentration-dependent manner (**Figure 1C** and [Supplementary Figure 1C](#)). The half-maximal inhibitory concentration (IC<sub>50</sub>) of ATO in LASCs from A549 cells was nearly 40  $\mu$ M, and the IC<sub>50</sub> of ATO in LASCs from NCI-H1975 cells was almost 24  $\mu$ M (**Figure 1C** and [Supplementary Figure 1C](#)). We detected the expression of major m6A-catalyzing genes in LASCs from A549 cells treated with ATO to analyze the roles of ATO in regulating m6A modification in LASCs. We found that the expression of m6A writers methyltransferase-like protein 14 (METTL14), METTL16, WTAP, and ZC3H13 (zinc finger CCCH domain-containing protein 13), as well as m6A erasers fat mass and obesity-associated gene (FTO) and alkylated DNA repair protein alkB homolog 5 (ALKBH5) genes in LASCs from A549 cells, were greatly reduced by ATO treatment using quantitative PCR assay (**Figure 1D**). Among them, ZC3H13 expression showed the greatest ATO treatment induced decrease (**Figure 1D**). Additionally, ATO treatment in LASCs from A549 cells remarkably downregulated the protein level of ZC3H13 (**Figure 1E**). Congruently, we observed via dot blot that the total m6A content in LASCs from A549 cells was significantly reduced by ATO treatment compared with the NC group (**Figure 1F**). Moreover, we revealed that ATO treatment significantly decreased the total m6A content and the expression of ZC3H13 in LASCs from NCI-H1975 cells compared with the negative control group ([Supplementary Figure 1D-F](#)). These results revealed that ATO treatment effectively suppressed cell proliferation and m6A modification in LASCs.

### *ATO promotes ferroptosis and suppresses stemness in LASCs*

We evaluated the influences of ATO treatment on the ferroptosis and stemness of LASCs to gain more insight into the mechanisms of LASCs regulation by ATO. We found by the tumorsphere formation assay that ATO treatment effectively repressed the sphere-forming capacities of LASCs compared with the NC group (**Figure 2A** and [Supplementary Figure 2A](#)). Additionally, flow cytometry revealed that ATO treatment greatly reduced the percentage of CD133+ LASCs compared with the NC group (**Figure 2B** and [Supplementary Figure 2B](#)). In contrast, we observed that ATO treatment significantly elevated the contents of reactive oxygen species (ROS) in the LASCs (**Figure 2C**). Similarly, the iron ion levels in the LASCs demonstrated substantial elevation after ATO treatment (**Figure 2D**). Correspondingly, ATO treatment greatly reduced the transcription level of the GPX4 gene in LASCs (**Figure 2E** and [Supplementary Figure 2C](#)). Consistently, our subsequent western blot revealed that ATO treatment significantly downregulated the protein abundances of GPX4 in LASCs (**Figure 2F** and [Supplementary Figure 2D](#)). Additionally, through transmission electron microscopy, we observed that ATO treatment caused significantly abnormal morphological alterations of mitochondria in LASCs, including mitochondrial membrane condensation, crystal membrane density elevation, shape irregularities, and mitochondrial crista reduction (**Figure 2G**). These results revealed that ATO can induce ferroptosis and repress stemness in LASCs.

### *ZC3H13 overexpression or ferrostatin-1 (Fer-1) treatment mitigates ATO-induced inhibition of LASCs stemness*

We overexpressed the m6A writer gene ZC3H13 in LASCs or inhibited ferroptosis progression in LASCs by Fer-1 to assess the mediating roles of m6A modification and ferroptosis in treatment induced LASCs stemness suppression. Through quantitative RT-PCR, we demonstrated that the mRNA levels of the ZC3H13 gene in LASCs under ATO treatment were greatly elevated by ZC3H13 gene overexpression, but not by Fer-1 treatment (**Figure 3A** and [Supplementary Figure 3A](#)). The following western blot assay revealed similar alterations of ZC3H13 proteins in LASCs treated with the

# Arsenic trioxide promotes ferroptosis in lung adenocarcinoma stem cells

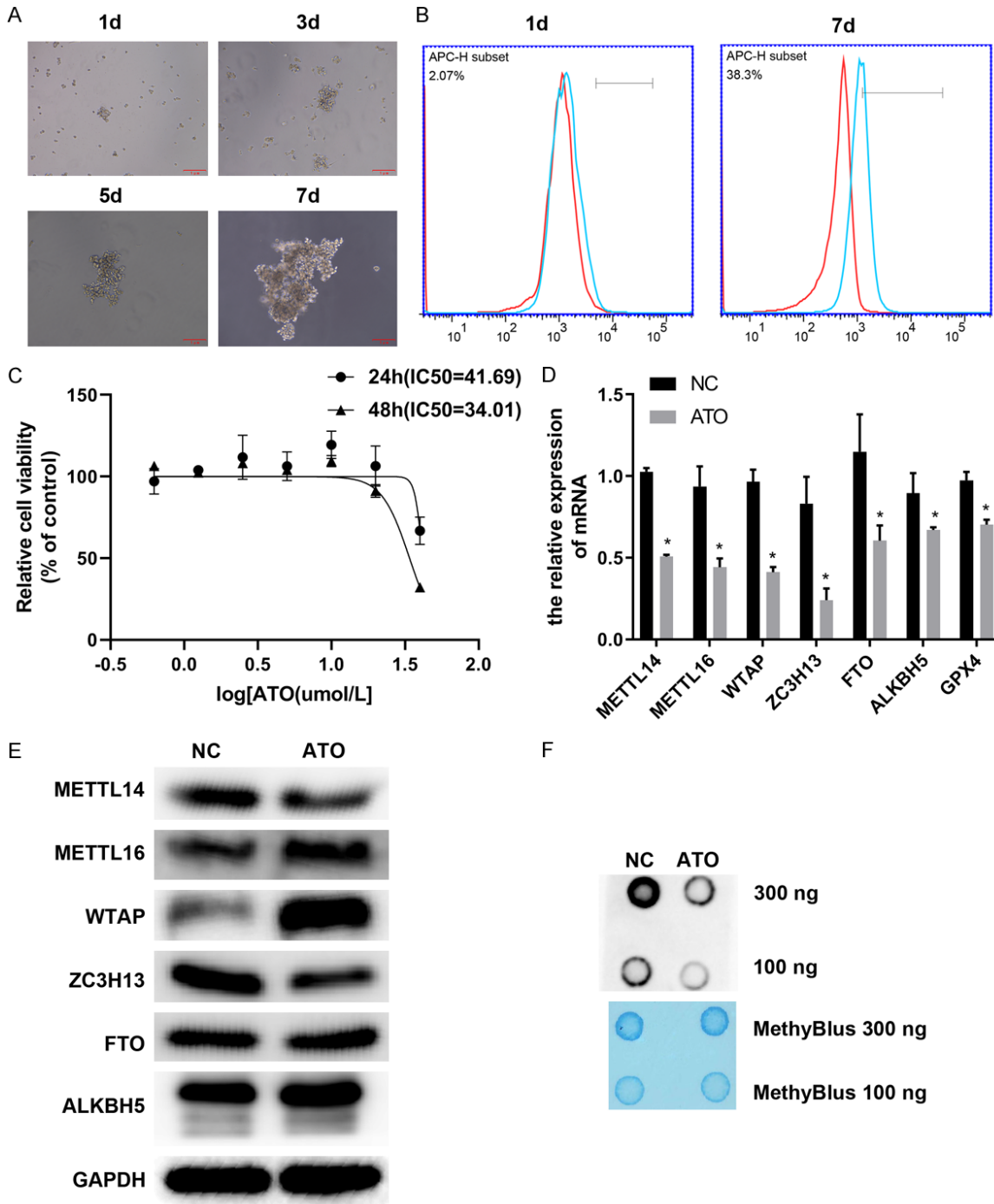


**Figure 1.** Inhibition of proliferation and m6A formation by ATO in LASCs from A549 cells. (A) Tumorsphere formation in A549 cells induced by treatment with the sphere formation medium. Tumor sphere formation after treatment for 1, 3, 5, and 7 days was evaluated using the sphere formation assay. (B) Increase in CD133-positive cells in A549 cells treated with sphere formation medium. The percentages of CD133+ cells were measured by flow cytometry. (C) Suppression of LASCs cell viability by ATO treatment for 24 or 48 h. LASCs from A549 cells were treated with 0, 0.625, 1.25, 2.5, 5, 10, 20, or 40 mM of ATO, followed by detection of cell viability by the CCK-8 method. (D and E) Effects of ATO treatment on the expression of m6A regulator genes in LASCs from A549 cells. The mRNA (D) and protein (E) levels of major m6A writers and erasers in LASCs from A549 cells were analyzed by quantitative RT-PCR and western blotting, respectively. (F) Decrease in total m6A content in LASCs from A549 cells induced by ATO treatment. The total m6A levels in LASCs from A549 cells were determined using the dot blot method. ATO: arsenic trioxide; LASCs: lung adenocarcinoma stem cells; NC: negative control; METTL14/16: methyltransferase-like protein 14/16; WTAP: Wilms' tumor 1-associating protein; ZC3H13: zinc finger CCCH domain-containing protein 13; FTO: fat mass and obesity-associated gene; ALKBH5: alkylated DNA repair protein alkB homolog 5; \* $P < 0.05$ .

## Arsenic trioxide promotes ferroptosis in lung adenocarcinoma stem cells

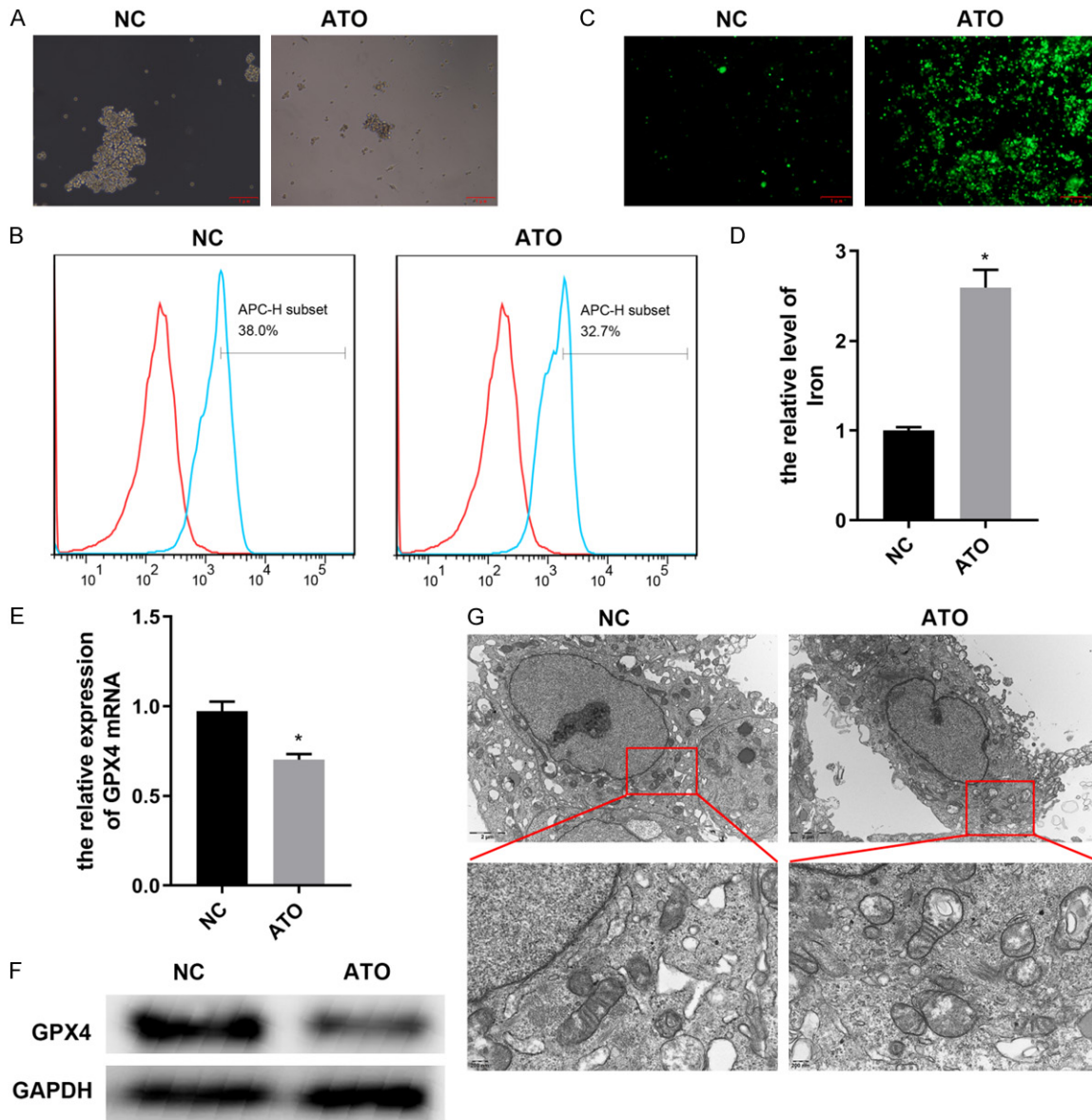


**Figure 2.** Modulation of LASCs from A549 cells ferroptosis and stemness by ATO. (A) Effects of ATO treatment on the sphere-forming capacities of LASCs. LASCs were treated with 20 mM of ATO for 48 h, and the capacity of tumor-sphere formation was assessed by the tumorsphere formation assay. (B) Decreased percentage of CD133-positive LASCs caused by ATO treatment. The percentages of CD133+ cells were analyzed using the flow cytometry method. (C) Promotion of ROS production in LASCs induced by ATO treatment. LASCs were treated with 20 mM of ATO for 24 h, and the ROS levels in LASCs were quantitated by fluorescence microscopy. (D) Increases in iron ion levels in LASCs after ATO treatment. The iron ion contents in the LASCs were detected by the colorimetric assay. (E and F) Inhibition of GPX4 gene expression by ATO treatment in LASCs. The mRNA (E) and protein (F) levels of GPX4 in LASCs were detected by quantitative RT-PCR and western blotting, respectively, after ATO treatment at 20 mM for 24 or 48 h. (G) Morphological aberrations in LASCs mitochondria induced by ATO treatment. The morphological features of mitochondria in LASCs were observed via transmission electron microscopy. LASCs: lung adenocarcinoma stem cells; NC: negative control; ATO: arsenic trioxide; GPX4: glutathione peroxidase 4; GAPDH: glyceraldehyde-3-phosphate dehydrogenase; \* $P < 0.05$ .

combination of ATO with Fer-1 or ZC3H13 over-expression (Figure 3B and Supplementary Figure 3B). Additionally, we revealed that the total m6A contents in the LASCs under ATO

treatment were greatly increased by ZC3H13 gene overexpression, but not influenced by Fer-1 treatment (Figure 3C). Importantly, we showed that tumor sphere formation in LASCs

## Arsenic trioxide promotes ferroptosis in lung adenocarcinoma stem cells

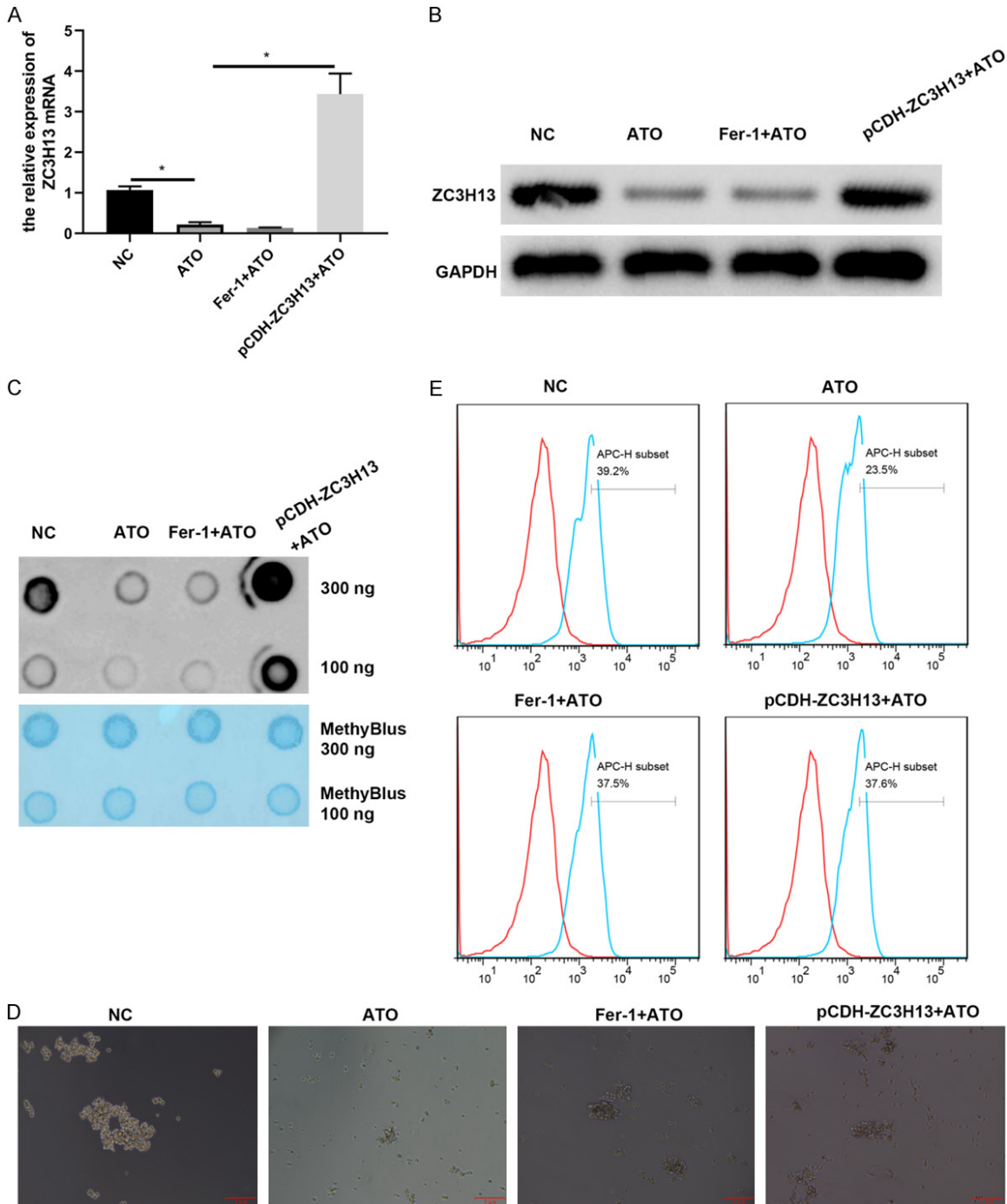


**Figure 3.** Effects of ZC3H13 overexpression and Fer-1 on the stemness of LASCs from A549 cells. **A.** ZC3H13 mRNA levels in LASCs that overexpress the ZC3H13 gene or treated with Fer-1. ZC3H13 mRNA levels in LASCs were analyzed by quantitative PCR. **B.** ZC3H13 protein abundances in LASCs with ZC3H13 gene overexpression or under the treatment. Western blotting was performed to assess ZC3H13 protein levels. **C.** Total m6A level changes in LASCs under ATO treatment combined with ZC3H13 overexpression or Fer-1 treatment. m6A levels in LASCs were detected via the dot blot method. **D.** Promotion of the sphere formation capacity of LASCs under ATO treatment by ZC3H13 overexpression or Fer-1 treatment. The tumorsphere-forming capacity of LASCs was assessed by the sphere formation assay. **E.** Recovery of the percentages of CD133-positive LASCs under ATO treatment by ZC3H13 gene overexpression or Fer-1 treatment. Percentages of CD133+ LASCs cells were quantitated by flow cytometry. Fer-1: ferrostatin-1; ZC3H13: zinc finger CCCH domain-containing protein 13; LASCs: lung adenocarcinoma stem cells; NC: negative control; ATO: arsenic trioxide; GAPDH: glyceraldehyde-3-phosphate dehydrogenase; \* $P < 0.05$ .

treated with ATO was greatly promoted by Fer-1 treatment or ZC3H13 overexpression compared with cells treated with ATO alone (**Figure 3D** and [Supplementary Figure 3C](#)). Consistently, we found significantly increased percentages of CD133-positive LASCs under ATO treatment by Fer-1 treatment or ZC3H13 overexpression, in contrast to LASCs treated with ATO alone (**Figure 3E** and [Supplementary Figure 3D](#)). These results indicated that LASCs stemness inhibition by ATO treatment was mediated by the repression of m6A modification and the promotion of ferroptotic cell death.

### *ZC3H13 overexpression abrogates LASCs ferroptosis enhancement caused by ATO treatment*

We subsequently assessed the alteration of ferroptosis status in LASCs with ZC3H13 overexpression under ATO treatment to validate the implication of m6A modification in regulating LASCs ferroptosis by ATO treatment. We observed that ROS production in LASCs treated with ATO was significantly lowered by Fer-1 treatment or ZC3H13 overexpression compared with LASCs treated with ATO alone (**Figure 4A**). Similarly, the iron ion levels in the LASCs under ATO treatment were greatly reduced by Fer-1 treatment or ZC3H13 overexpression compared with the ATO treatment (**Figure 4B**). Moreover, we observed by both quantitative RT-PCR and western blot assays that Fer-1 treatment or ZC3H13 overexpression remarkably promoted GPX4 gene expression in LASCs treated with ATO, in contrast to the ATO treatment group (**Figure 4C, 4D** and [Supplementary Figure 4A, 4B](#)). Additionally, our transmission electron microscopy method confirmed that ATO treatment induced abnormal morphological alterations of mitochondria in LASCs which were substantially alleviated by ZC3H13 overexpression or Fer-1 treatment (**Figure 4E**).

### *Fer-1 treatment mitigates alterations in LASCs ferroptosis and stemness induced by si-ZC3H13*

We assessed the changes in ferroptosis and stemness of LASCs under si-ZC3H13-1 (or si-ZC3H13-2) and Fer-1 treatment to further analyze the roles of ferroptosis in improving m6A-regulated LASCs stemness. The quantitative PCR method revealed that si-ZC3H13-1 (or si-

ZC3H13-2) greatly downregulated the mRNA levels of the ZC3H13 gene in LASCs, which the combination of Fer-1 treatment could not change (**Figure 5A** and [Supplementary Figure 5A](#)). Corresponding alterations of the ZC3H13 proteins in LASCs were observed after treatment with si-ZC3H13-1 (or si-ZC3H13-2) and Fer-1 (**Figure 5B** and [Supplementary Figure 5B](#)). Consistently, we found that si-ZC3H13-1 (or si-ZC3H13-2) transfection substantially repressed the total m6A content in the LASCs, which could not be recovered by Fer-1 treatment (**Figure 5C**). Moreover, si-ZC3H13-1 (or si-ZC3H13-2) transfection greatly increased the total ROS content in LASCs, which the combination of Fer-1 treatment significantly abrogated (**Figure 5D**). Furthermore, si-ZC3H13-1 (or si-ZC3H13-2) transfection remarkably elevated the total iron ion levels in the LASCs, which Fer-1 treatment had substantially inhibited (**Figure 5E**). In contrast, si-ZC3H13-1 (or si-ZC3H13-2) transfection significantly downregulated the GPX4 gene expression in LASCs, which the combination of Fer-1 treatment has effectively elevated (**Figure 5F, 5G** and [Supplementary Figure 5A, 5B](#)). Additionally, si-ZC3H13-1 (or si-ZC3H13-2) transfection induced abnormal mitochondrial changes in LASCs, which the combination of Fer-1 treatment has significantly alleviated (**Figure 5H**). Conversely, we observed that si-ZC3H13-1 (or si-ZC3H13-2) transfection greatly reduced both the sphere-forming capacity and CD133+ cell percentages in the LASCs, which the combination of Fer-1 treatment has greatly recovered (**Figure 5I, 5J** and [Supplementary Figure 5C, 5D](#)). These results confirmed that ZC3H13-mediated m6A modification enhances LASCs stemness by inhibiting ferroptosis.

### *Interference with ZC3H13 further inhibited the ATO-induced LASCs stemness inhibition*

ATO downregulates ZC3H13 expression, and interference with ZC3H13 combined with ATO treatment can further decrease the regulation of ZC3H13 mRNA and protein expression (**Figure 6A, 6B** and [Supplementary Figure 6A, 6B](#)). ATO downregulated the modification level of total RNA m6A, and interference with ZC3H13 combined with ATO treatment further downregulated the modification level of total RNA m6A (**Figure 6C**). ATO inhibited stem cell tumor cluster formation, and interference with ZC3H13 combined with ATO treatment further

## Arsenic trioxide promotes ferroptosis in lung adenocarcinoma stem cells

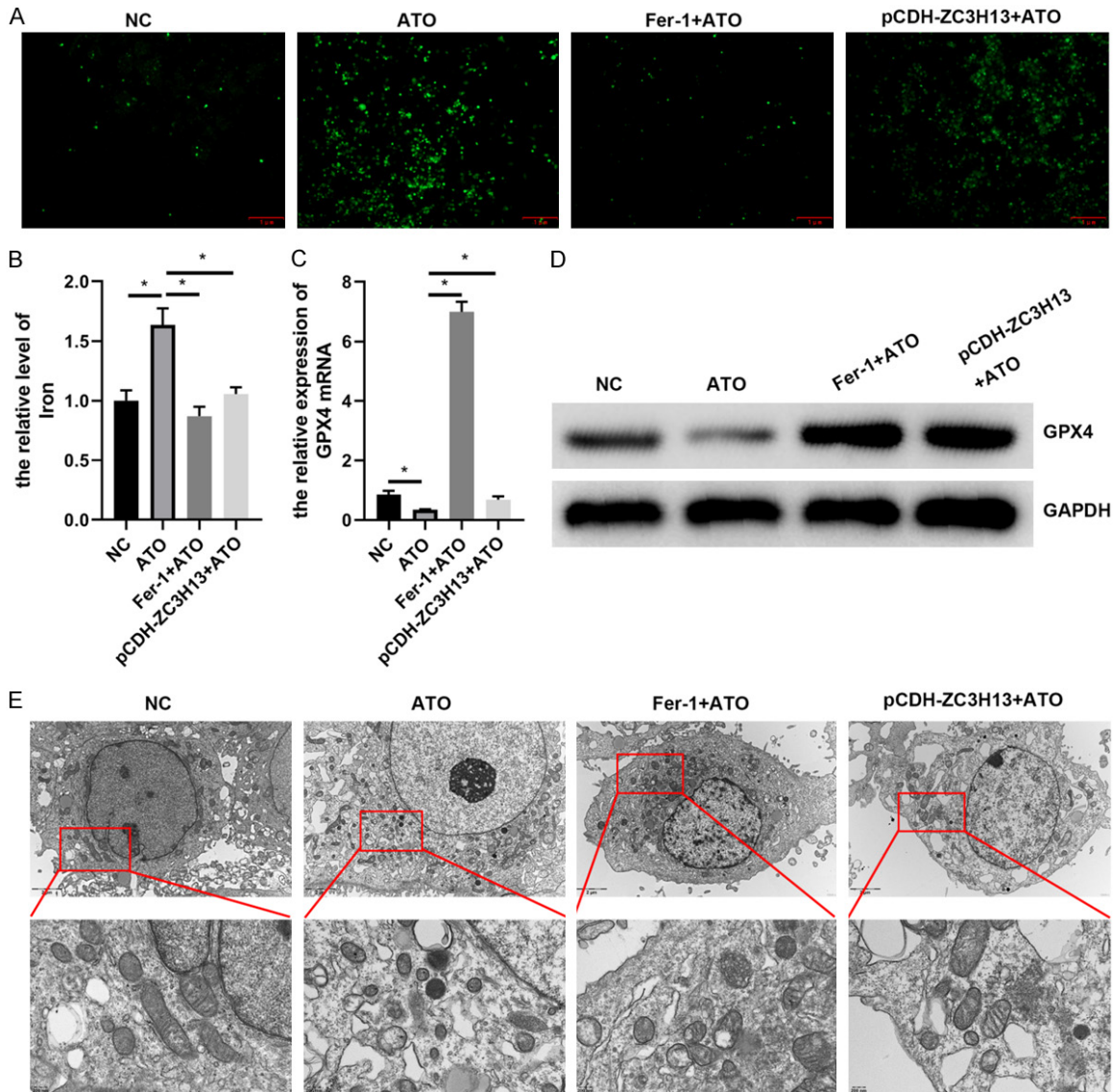


**Figure 4.** Alleviation of ATO-induced LASCs ferroptosis by ZC3H13 overexpression. (A) ROS content downregulation in LASCs from A549 cells treated with ATO by ZC3H13 overexpression or Fer-1 treatment. ROS levels in LASCs from A549 cells were determined using fluorescence microscopy. (B) Decrease in iron ion content in LASCs from A549 cells under ATO treatment by Fer-1 treatment or ZC3H13 overexpression. Iron ion contents in LASCs from A549 cells were measured using the colorimetric method. (C and D) Elevated GPX4 gene expression in LASCs from A549 cells under ATO treatment by Fer-1 treatment or ZC3H13 overexpression. GPX4 mRNA (C) or protein (D) levels in LASCs from A549 cells were detected by quantitative PCR and western blotting, respectively. (E) The alleviation of ATO-induced LASCs mitochondrial aberrations by ZC3H13 overexpression or Fer-1 treatment. LASCs were obtained from A549 cells. LASCs: lung adenocarcinoma stem cells; NC: negative control; ATO: arsenic trioxide; Fer-1: ferrostatin-1; ZC3H13: zinc finger CCCH domain-containing protein 13; GPX4: glutathione peroxidase 4; GAPDH: glyceraldehyde-3-phosphate dehydrogenase; \* $P < 0.05$ .

decreased stem cell tumor cluster formation (Figure 6D and Supplementary Figure 6C). ATO inhibited the proportion of CD133-positive stem cells, and interference with ZC3H13 combined with ATO treatment further decreased the proportion of CD133-positive stem cells

(Figure 6E and Supplementary Figure 6D). Moreover, ATO decreased GPX4 expression at the mRNA and protein levels, and interference with ZC3H13 combined with ATO treatment further inhibited the mRNA and protein expression of GPX4 (Supplementary Figure 6A, 6B). The

# Arsenic trioxide promotes ferroptosis in lung adenocarcinoma stem cells

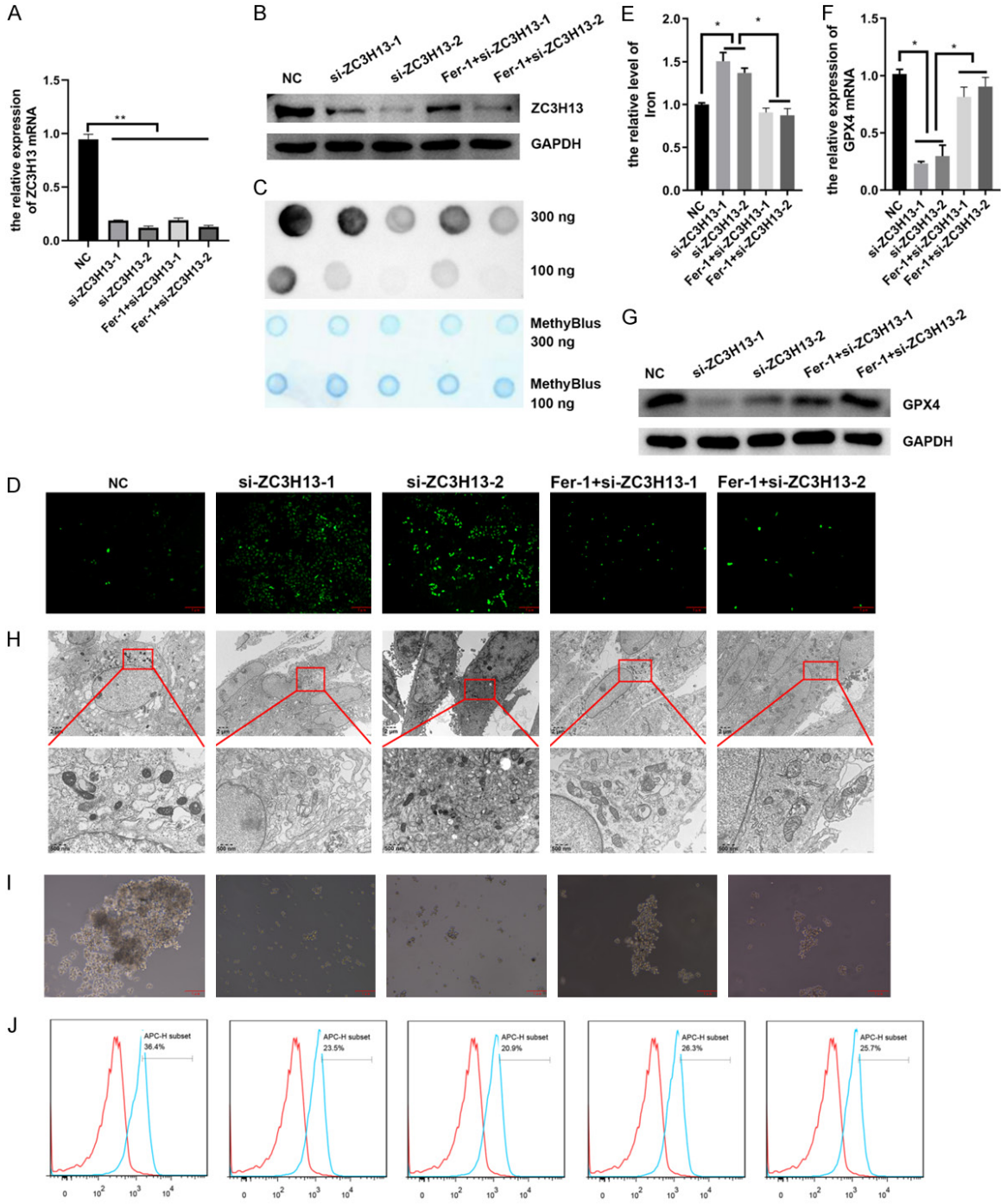


**Figure 5.** Abrogation of si-ZC3H13-induced ferroptosis enhancement and stemness inhibition in LASCs from A549 cells by Fer-1 treatment. (A and B) Expression levels of ZC3H13 gene in LASCs treated with si-ZC3H13-1 (or si-ZC3H13-2) and Fer-1. ZC3H13 mRNA (A) and protein (B) levels in LASCs were quantitated by quantitative RT-PCR and western blotting, respectively. (C) Changes in total m6A modification levels in LASCs treated with a combination of si-ZC3H13-1 (or si-ZC3H13-2) and Fer-1. Total m6A levels in LASCs were analyzed using the dot blot assay. (D) Effects of Fer-1 treatment on ROS content in LASCs transfected with si-ZC3H13-1 (or si-ZC3H13-2). Fluorescence microscopy was used for the quantitation of ROS content in LASCs. (E) Iron ion level downregulation in LASCs treated with si-ZC3H13-1 (or si-ZC3H13-2) by Fer-1 treatment. The iron ion contents in LASCs were compared using the colorimetric method. (F and G) Promotion of GPX4 gene expression by Fer-1 treatment in LASCs with ZC3H13 knockdown by si-ZC3H13-1 (or si-ZC3H13-2). The mRNA (F) and protein (G) levels of the GPX4 gene in LASCs were detected by quantitative PCR and western blotting, respectively. (H) Modulation of mitochondrial functions by Fer-1 treatment in LASCs with silenced ZC3H13 expression. Morphological alterations of mitochondria in LASCs were assessed by transmission electron microscopy. (I) Recovery of the sphere-forming capacity of ZC3H13-silenced LASCs

## Arsenic trioxide promotes ferroptosis in lung adenocarcinoma stem cells

by Fer-1 treatment. Tumor sphere formation by LASCs was evaluated using the sphere formation assay. (J) Elevation of CD133-positive cell percentages in ZX3H13-silenced LASCs by Fer-1 treatment. Flow cytometry was performed to quantify CD133-positive LASCs percentages. ZC3H13: zinc finger CCCH domain-containing protein 13; LASCs: lung adenocarcinoma stem cells; NC: negative control; si-ZC3H13-1: siRNA fragment 1 of ZC3H13; si-ZC3H13-2: siRNA fragment 2 of ZC3H13; Fer-1: Ferrostatin-1; GAPDH: glyceraldehyde-3-phosphate dehydrogenase; GPX4: glutathione peroxidase 4; \* $P < 0.05$ .

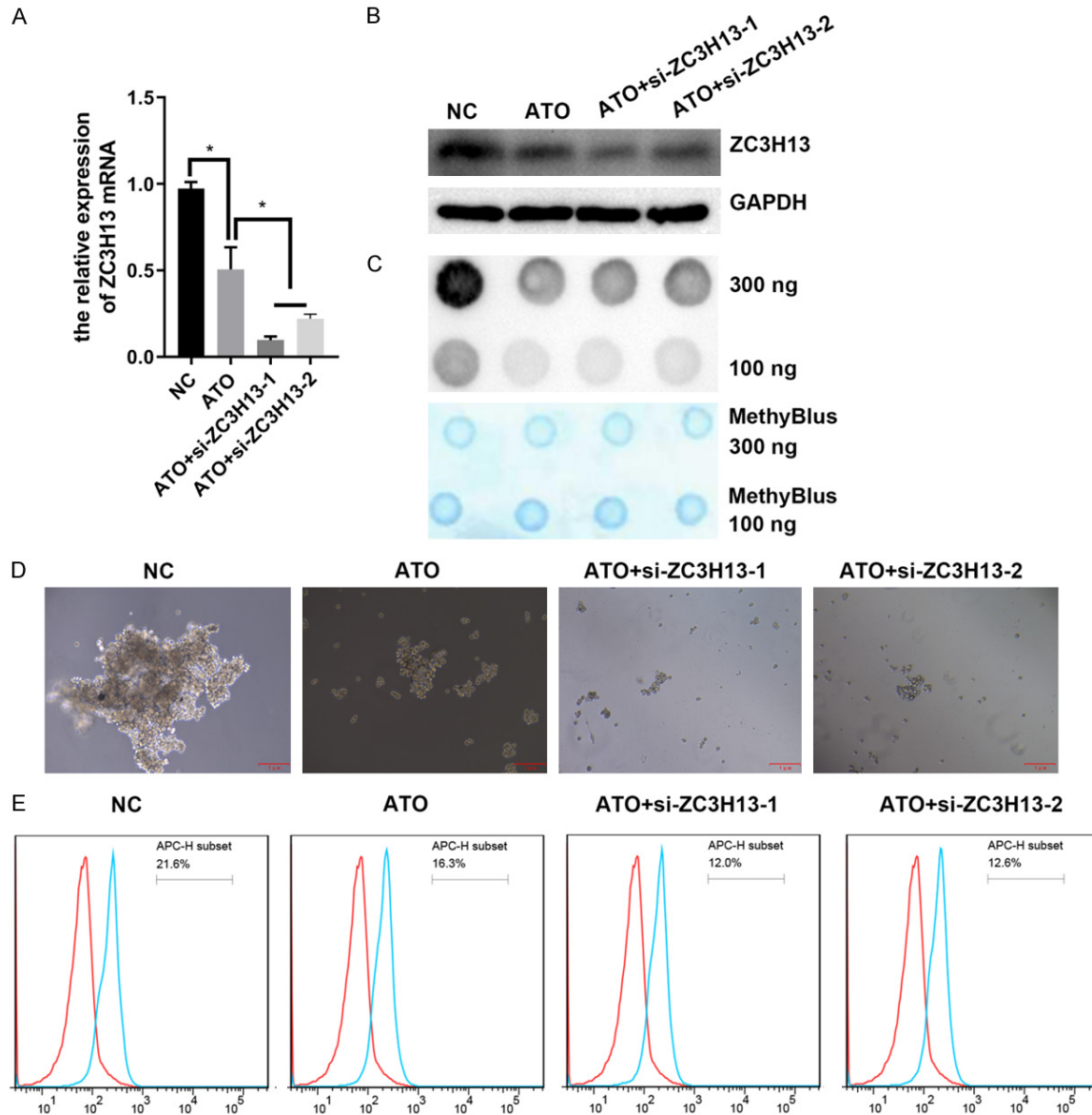


**Figure 6.** Effects of interference with ZC3H13 on the stemness of LASCs from A549 cells. A. ZC3H13 mRNA levels in LASCs with ZC3H13 combined with ATO treatment. ZC3H13 mRNA levels in LASCs were analyzed by quantitative PCR. B. ZC3H13 protein abundances in LASCs with ZC3H13 combined with ATO treatment. Western blotting was performed to evaluate ZC3H13 protein levels. C. Alterations of total m6A levels in LASCs interference with ZC3H13 combined with ATO treatment. m6A levels in LASCs were detected via the dot blot method. D. Promotion of the sphere formation capacity of LASCs interference with ZC3H13 combined with ATO treatment. The tumorsphere-forming capacity of LASCs was evaluated using the sphere formation assay. E. Percentages of CD133-positive LASCs after interference with ZC3H13 combined with ATO treatment. Percentages of CD133+ LASCs cells were quantitated by flow cytometry. ZC3H13: zinc finger CCCH domain-containing protein 13; LASCs: lung adenocarcinoma stem cells; NC: negative control; si-ZC3H13-1: siRNA fragment 1 of ZC3H13; si-ZC3H13-2: siRNA fragment 2 of ZC3H13; ATO: arsenic trioxide; GAPDH: glyceraldehyde-3-phosphate dehydrogenase; \* $P < 0.05$ .

results revealed that ATO inhibits LASCs stemness and ferroptosis, and interference with ZC3H13 combined with ATO treatment further decreases LASCs stemness and ferroptosis.

### *Interference with ZC3H13 promotes LASCs ferroptosis*

ATO promoted ROS activity, and interference with ZC3H13 combined with ATO treatment further enhanced ROS activity (**Figure 7A**). ATO upregulated intracellular iron concentration, and interference with ZC3H13 combined with ATO treatment further increased the regulation of intracellular iron concentration (**Figure 7B**). ATO inhibited GPX4 expression, and interference with ZC3H13 combined with ATO treatment further repressed GPX4 mRNA and protein expression (**Figure 7C, 7D**). ATO could damage mitochondria, whereas interference with ZC3H13 combined with ATO treatment could further damage mitochondria (**Figure 7E**). The results demonstrated that ATO can promote ferroptosis and that interference with ZC3H13 combined with ATO treatment can further enhance ferroptosis.

### *ZC3H13 overexpression mitigated the LASCs tumorigenicity inhibition by ATO treatment*

We finally applied a cancer cell line-based xenograft model to assess the tumorigenicity of LASCs to further validate the functions of ZC3H13-mediated m6A modification in inhibiting LUAD development by ATO. We observed significantly lower tumor volumes that developed from LASCs in naked mice treated with ATO than those in the NC group, whereas ZC3H13 overexpression partially recovered tumor volumes in mice treated with ATO (**Figure 8A, 8B**). Similarly, ATO treatment significantly reduced the weights of tumors formed in naked mice, which were partially recovered by ZC3H13 overexpression in LASCs (**Figure 8C**). Additionally, we revealed that the expression of the ZC3H13 gene in the tumor tissues of the ATO group was remarkably lower than that in the NC group, but ZC3H13 overexpression in LASCs significantly elevated the expression of ZC3H13 in tumor tissues formed in the naked mice (**Figure 8D**). The abundance of ZC3H13 protein in the tumors formed in naked mice was also markedly increased by ZC3H13 gene overexpression in LASCs (**Figure 8E**).

More importantly, we found a significantly lower total m6A modification in the tumors of the ATO group than that in the NC group, which was then substantially elevated by ZC3H13 overexpression in the LASCs (**Figure 8F**). Our subsequent immunofluorescence assay revealed that the number of CD133+ cells in tumor tissues of the ATO group was significantly less than that of the NC group, which was then elevated by ZC3H13 overexpression in LASCs (**Figure 8G**). In contrast, the ROS contents in the tumors of the ATO group were significantly higher than those of the NC group, which was then greatly reduced by ZC3H13 overexpression in LASCs (**Figure 8H**). Similar changes in iron ion levels were detected in tumors derived from ZC3H13-overexpressing LASCs in naked mice treated with ATO (**Figure 8I**). Additionally, we revealed that both the mRNA and protein GPX4 gene levels in tumors of the ATO group were effectively decreased by ATO treatment in naked mice, which were then substantially elevated by ZC3H13 overexpression in LASCs (**Figure 8J, 8K**). Together, these results indicated that ATO could effectively impair the tumorigenicity of LASCs in naked mice by inhibiting ZC3H13 expression.

## Discussion

ATO was applied for the clinical treatment of multiple human disorders in ancient China and other countries for a long time [6, 20]. However, the greatest attention has only been paid to this chemical drug since the recent discovery of its potency in suppressing APL and other malignancy diseases [6, 20, 21]. The possibility of ATO in regulating cancer stem cells of LUAD, as well as the underlying mechanisms, remains elusive despite extensive research revealing the potency of ATO in inhibiting lung cancer development and progression. This study revealed that ATO effectively inhibited the stemness of LASCs, accompanied by ferroptosis improvement and m6A modification inhibition. Our subsequent investigations clarified that LASCs stemness inhibition by ATO mediated the suppression of ZC3H13 expression to reduce m6A modification, thereby enhancing ferroptosis. Furthermore, we revealed that ZC3H13-mediated m6A modification improves the stemness of LASCs by inhibiting ferroptosis. Finally, we confirmed, using a CDX model, that ATO treatment substantially repressed the

## Arsenic trioxide promotes ferroptosis in lung adenocarcinoma stem cells

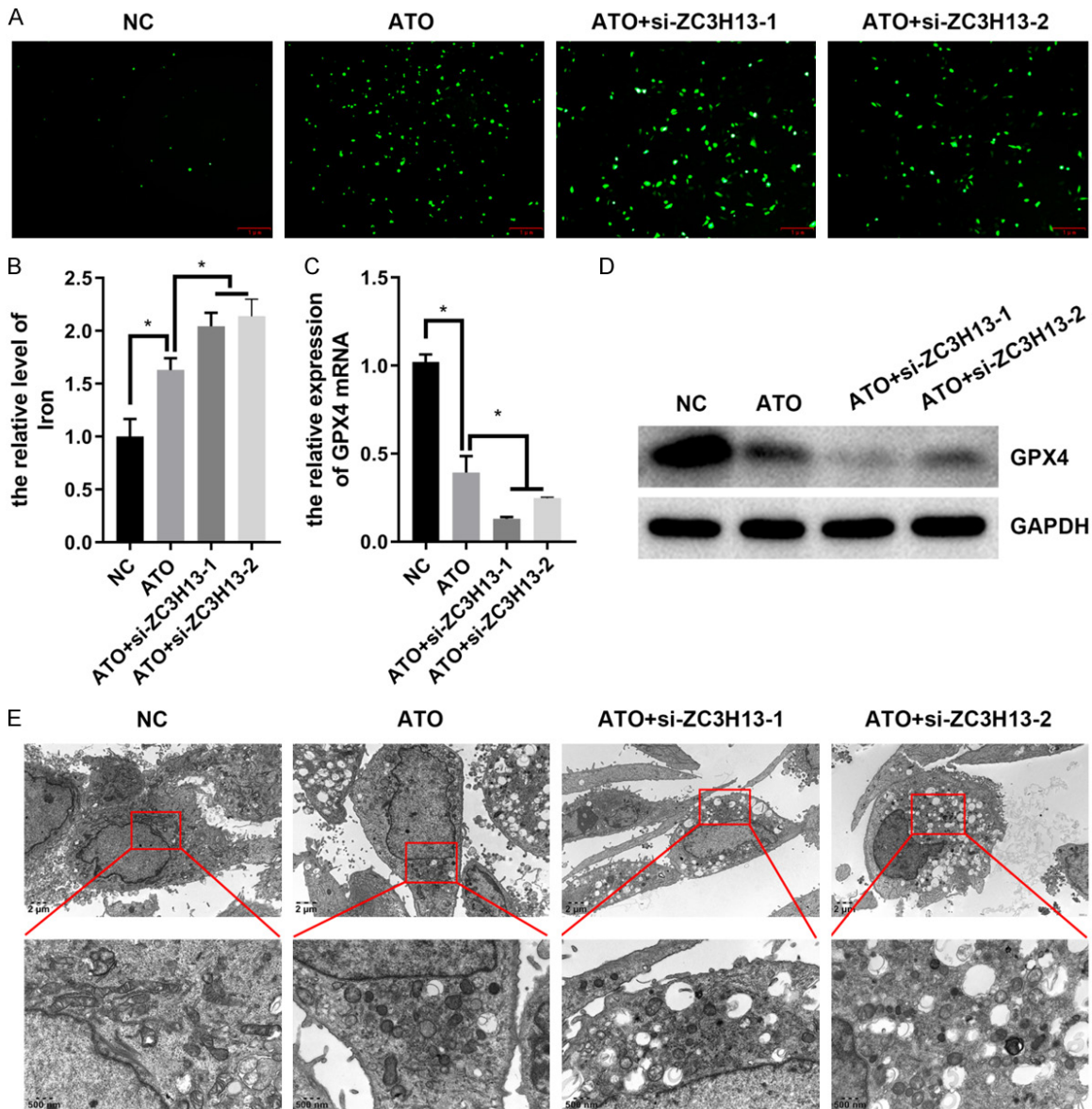


**Figure 7.** Effects of interference with ZC3H13 on ferroptosis in LASCs from A549 cells. (A) ROS content downregulation in LASCs that interfere with ZC3H13 combined with ATO treatment. ROS levels in LASCs were determined using fluorescence microscopy. (B) Decrease in iron ion contents in LASCs that interfere with ZC3H13 combined with ATO treatment. Iron ion contents in LASCs were measured using the colorimetric method. (C and D) GPX4 gene or protein expression in LASCs that interfere with ZC3H13 combined with ATO treatment. GPX4 mRNA (C) or protein (D) levels in LASCs were detected by quantitative PCR and western blotting, respectively. (E) Enhancement of ATO-induced LASCs mitochondrial aberrations by interference with ZC3H13 combined with ATO treatment. LASCs: lung adenocarcinoma stem cells; NC: negative control; si-ZC3H13-1: siRNA fragment 1 of ZC3H13; si-ZC3H13-2: siRNA fragment 2 of ZC3H13; ATO: arsenic trioxide; ZC3H13: zinc finger CCCH domain-containing protein 13; GPX4: glutathione peroxidase 4; GAPDH: glyceraldehyde-3-phosphate dehydrogenase; \* $P < 0.05$ .

tumorigenicity of LASCs by inhibiting ZC3H13 expression to modulate m6A formation and ferroptosis progression. These observations indicate that ATO inhibits LUAD progression by regulating m6A modification and ferroptosis to suppress LASCs stemness.

Cancer stem cells (CSCs) refer to the specialized subgroup of cancer cells featuring high tumorigenic properties such as high invasion, migration, high self-renewal, and differentiation capacities [22-24]. Since their first discovery in the 1970s, CSCs have become a research

# Arsenic trioxide promotes ferroptosis in lung adenocarcinoma stem cells

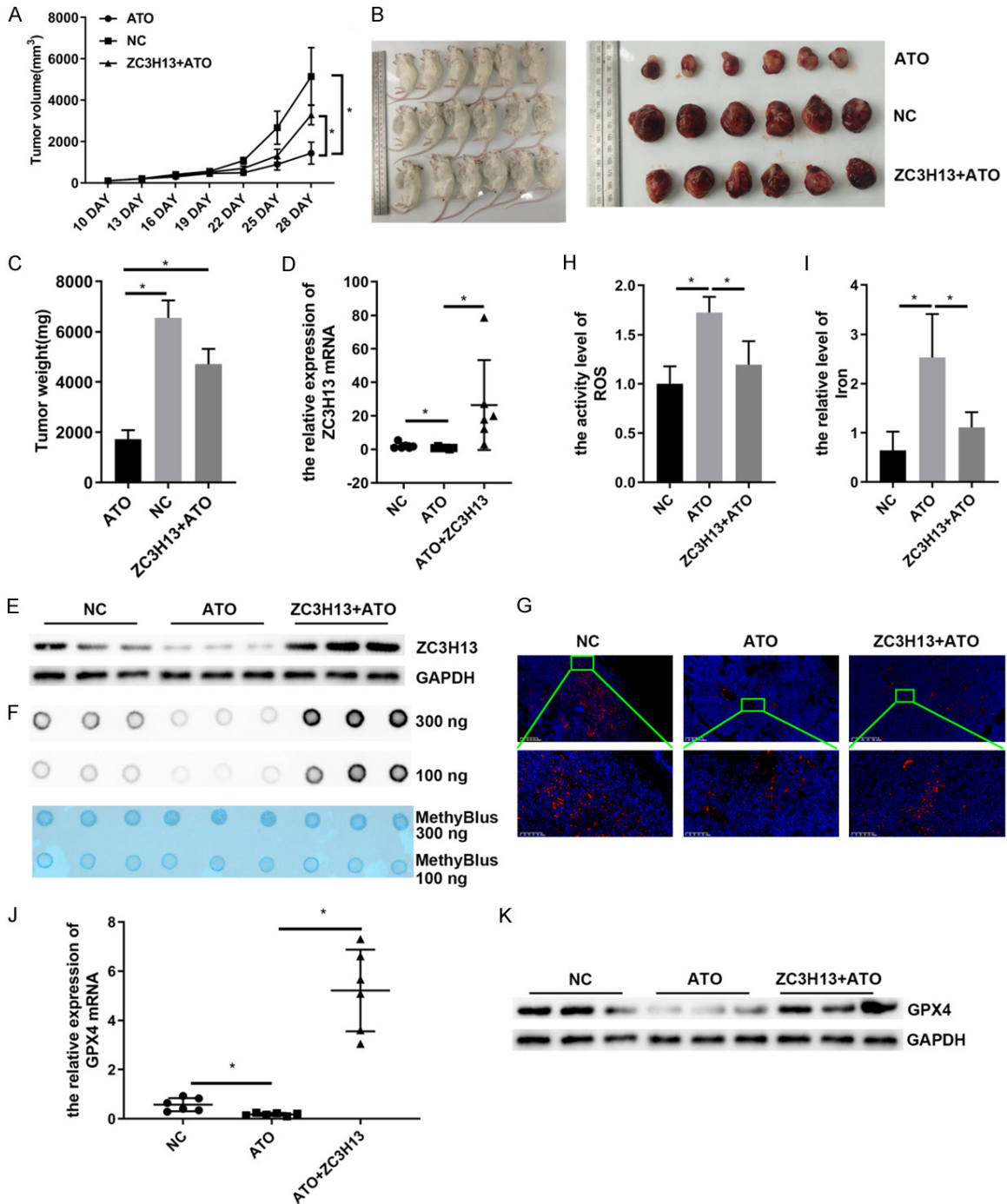


**Figure 8.** ATO impaired LASCs tumorigenicity by inhibiting ZC3H13 to promote ferroptosis. (A-C) Effect of ZC3H13 overexpression on the volumes and weights of tumors formed in ATO-treated naked mice. The volume (A and B) and weights (C) of tumors formed in naked mice were measured weekly after LASCs from A549 cells injection, which lasted for four consecutive weeks. (D and E) Alterations in ZC3H13 gene expression in tumors derived from ZC3H13-overexpressing LASCs in naked mice treated with ATO. ZC3H13 mRNA and protein levels in tumors were detected by quantitative PCR and western blotting, respectively. (F) Elevation of total m6A content in tumors developed from ZC3H13-overexpressing LASCs in naked mice treated with ATO. Total m6A levels in tumor tissues were analyzed using the dot bot. (G) Changes in CD133+ cells in tumors derived from ZC3H13-overexpressing LASCs in naked mice treated with ATO. Immunofluorescence was performed to assess CD133+ cells in mice tissues. (H) ROS contents in tumor tissues developed from ZC3H13-overexpressing LASCs in naked mice under ATO treatment. (I) Influence of ZC3H13 overexpression on the iron ion level of tumor tissues in mice treated with ATO. Iron ion levels in tumor tissues were measured using the colorimetric method. (J and K) ZC3H13 overexpression-induced alterations of GPX4 expression in tumors developed from LASCs in naked mice. GPX4 mRNA and protein levels in tumor tissues

## Arsenic trioxide promotes ferroptosis in lung adenocarcinoma stem cells

were measured by quantitative PCR and western blotting, respectively. LASCs: lung adenocarcinoma stem cells; NC: negative control; ATO: arsenic trioxide; ZC3H13: zinc finger CCCH domain-containing protein 13; GPX4: glutathione peroxidase 4; GAPDH: glyceraldehyde-3-phosphate dehydrogenase; \* $P < 0.05$ .

hotspot during the past decades in the cancer biology field due to the elucidation of CSCs as key drivers and main mediators of cancer initiation, high metastasis rates, immune escape, chemotherapy resistance, and disease relapse [22, 25]. Therefore, developing effective inhibitors, specifically targeting CSCs, has long been regarded as a promising strategy for obtaining new therapeutic drugs with a high possibility of improving long-term outcomes. Previous research has revealed that ATO inhibits CSC activity in hepatocellular carcinoma by modulating NF- $\kappa$ B signaling or targeting the Minichromosome maintenance protein 7 (MCM7) complex [26, 27]. Additionally, ATO could repress the activities of CSLC in lung cancer [11], but its CSC regulation in LUAD remains unknown. This study confirmed, for the first time, that ATO significantly inhibited LASCs stemness, as evidenced by the remarkable decreases in sphere-forming capacity and CD133+ cell percentages, indicating the high possibility of ATO being applied as an effective anti-LUAD treatment, especially for those with strong chemotherapy resistance.

As introduced above, ferroptosis is a newly characterized type of programmed cell death characterized by the involvement of phospholipid peroxidation, ROS overproduction, and iron ion accumulation [12, 14]. Additionally, ferroptosis program progression has been usually evaded in the initiation and development of various cancer types, including lung cancer [16, 17]. In contrast, ferroptosis has recently repressed the invasiveness, metastasis, and chemotherapy tolerance of many types of CSCs, including ovarian, colorectal, and breast cancers [28-30]. However, the roles of ferroptosis in LUAD pathogenesis in cancer stem cell regulation remain largely unknown. This study revealed that ATO treatment induced significant ROS production and iron ion accumulation in LASCs, demonstrating that ATO can induce the ferroptosis program in LASCs. Moreover, GPX4 generally protects cells against ferroptosis because of its capability to repress phospholipid peroxides; thus, GPX4 inhibition has been applied as a common ferroptosis biomarker [31, 32]. Additionally, we observed that ATO

treatment significantly decreased GPX4 expression in LASCs. Furthermore, the inhibition of ferroptosis development using Fer-1 alleviated the suppression of sphere formation and CD133+ cell percentage in LASCs by ATO treatment, providing strong evidence of the mediating roles of ferroptosis in ATO-induced LASCs inhibition, which provides clues for the potential application of other ferroptosis regulators in LUAD treatment.

N6-methyladenosine (m6A) is a key type of internal transcript modification catalyzed by multiple methyltransferases, such as METTL3/14, WTAP, ZC3H13, and vir like m6A methyltransferase associated, which can be reversed by several demethylases, including FTO and ALKBH5 [33, 34]. M6A modification serves as an important layer of the post-transcriptional mechanism regulating eukaryotic gene expression [35], which is closely associated with multiple physiological processes and disease development, including lung cancer, because of its significant impacts on RNA splicing, stability and degradation, translation initiation, and elongation [33, 35, 36]. In particular, m6A modification promotes cell proliferation and LUAD metastasis by modulating the Wnt/ $\beta$ -catenin signaling cascades [37]. Other extensive research in recent years has also supported the significant implication of m6A modification in LUAD pathogenesis [38-40]. More importantly, m6A catalyzed by METTL3 inhibited ferroptosis to improve LUAD development and progression [19]. In this study, we revealed that ATO treatment significantly repressed m6A writer ZC3H13 expression and m6A formation in LASCs, which essentially mediated the functions of ATO in promoting ferroptosis and repressing stemness in LASCs. Additionally, an *in vivo* tumorigenicity assay in naked mice further validated the mediating roles of ZC3H13-induced m6A modification and ferroptosis in LUAD inhibition by ATO treatment. These results revealed the feasibility of targeting m6A modification in CSCs as a new strategy for malignant disease prevention.

In summary, we explored the anti-LUAD pharmaceutical mechanism of ATO using a cellular

# Arsenic trioxide promotes ferroptosis in lung adenocarcinoma stem cells

LASCs model in this study and demonstrated that ATO effectively suppressed LASCs proliferation and stemness through inhibition of ZC3H13-mediated m6A modification to promote the ferroptosis program. These observations provided new insights into the molecular mechanism underlying the inhibitory effects of ATO on LUAD development and progression, which also guided the application of ATO and other m6A modifiers in the clinical management of patients with lung cancer.

## Acknowledgements

This study was supported by the National Natural Science Foundation of China: 82000329 and 82074424; the Guangzhou Basic Research Program City School (Institute) Joint Funding Project: 202201020244; the Guangdong Second People's Hospital Lift Project Special Fund: TJGC-2022005; the Guangdong Basic and Applied Basic Research Foundation: 2019A1515110139; the Guangdong Natural Science Foundation: 2020A1515010182; the Science Foundation of Guangdong Second Provincial General Hospital: YQ2018-012 and YQ2017-019; the Project of Administration of Traditional Chinese Medicine of Guangdong Province of China: 20211021; the Doctoral Workstation Foundation of Guangdong Second Provincial General Hospital: 2019BSGZ004; the 3D Printing Clinical Application Foundation of Guangdong Second Provincial General Hospital: 3D-B2020008; and the Key Project of Guangdong and Ganzi Hospital Pair Support Plan: Gan Fagai (2019) No. 181.

## Disclosure of conflict of interest

None.

**Address correspondence to:** Dr. Wen Yan, Department of Oncology, The Second People's Hospital of Guangdong Province, No. 466 Xingang Middle Road, Haizhu District, Guangzhou 510310, Guangdong, China. Tel: +86-020-89168093; E-mail: yanw@gd2h.org.cn; Dr. Ruqin Chen, Department of Traditional Chinese Medicine, The Second People's Hospital of Guangdong Province, No. 466 Xingang Middle Road, Haizhu District, Guangzhou 510310, Guangdong, China. Tel: +86-020-89168093; E-mail: chenrq36@sina.com

## References

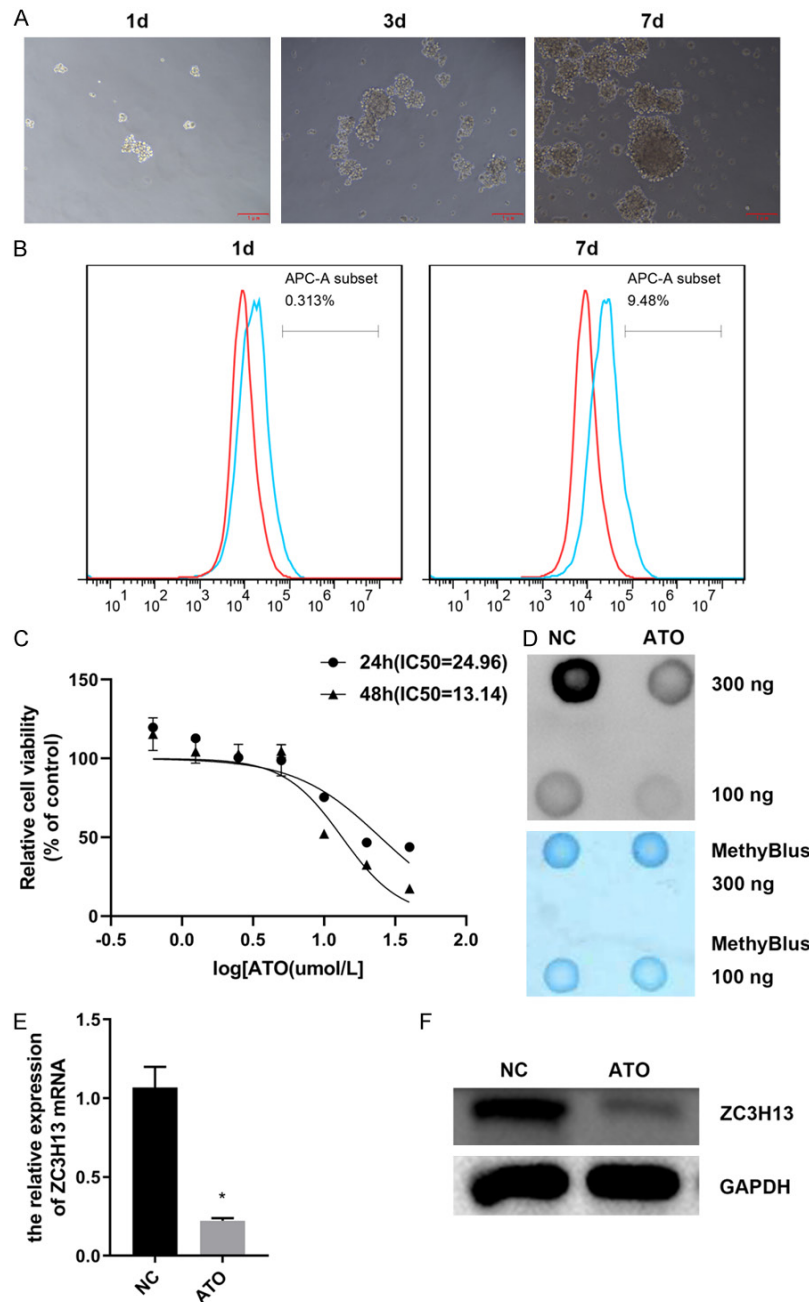
[1] Denisenko TV, Budkevich IN and Zhivotovsky B. Cell death-based treatment of lung adenocarcinoma. *Cell Death Dis* 2018; 9: 117.

- [2] Barta JA, Powell CA and Wisnivesky JP. Global epidemiology of lung cancer. *Ann Glob Health* 2019; 85: 8.
- [3] Chalela R, Curull V, Enriquez C, Pijuan L, Bellosillo B and Gea J. Lung adenocarcinoma: from molecular basis to genome-guided therapy and immunotherapy. *J Thorac Dis* 2017; 9: 2142-2158.
- [4] Inamura K. Clinicopathological characteristics and mutations driving development of early lung adenocarcinoma: tumor initiation and progression. *Int J Mol Sci* 2018; 19: 1259.
- [5] Saito M, Shiraishi K, Kunitoh H, Takenoshita S, Yokota J and Kohno T. Gene aberrations for precision medicine against lung adenocarcinoma. *Cancer Sci* 2016; 107: 713-720.
- [6] Hoonjan M, Jadhav V and Bhatt P. Arsenic trioxide: insights into its evolution to an anticancer agent. *J Biol Inorg Chem* 2018; 23: 313-329.
- [7] Huang W and Zeng YC. A candidate for lung cancer treatment: arsenic trioxide. *Clin Transl Oncol* 2019; 21: 1115-1126.
- [8] Yang MH, Zang YS, Huang H, Chen K, Li B, Sun GY and Zhao XW. Arsenic trioxide exerts anti-lung cancer activity by inhibiting angiogenesis. *Curr Cancer Drug Targets* 2014; 14: 557-566.
- [9] Lam SK, Li YY, Zheng CY, Leung LL and Ho JC. E2F1 downregulation by arsenic trioxide in lung adenocarcinoma. *Int J Oncol* 2014; 45: 2033-2043.
- [10] Lam SK, Mak JC, Zheng CY, Li YY, Kwong YL and Ho JC. Downregulation of thymidylate synthase with arsenic trioxide in lung adenocarcinoma. *Int J Oncol* 2014; 44: 2093-2102.
- [11] Chang KJ, Yang MH, Zheng JC, Li B and Nie W. Arsenic trioxide inhibits cancer stem-like cells via down-regulation of Gli1 in lung cancer. *Am J Transl Res* 2016; 8: 1133-1143.
- [12] Jiang X, Stockwell BR and Conrad M. Ferroptosis: mechanisms, biology and role in disease. *Nat Rev Mol Cell Biol* 2021; 22: 266-282.
- [13] Li J, Cao F, Yin HL, Huang ZJ, Lin ZT, Mao N, Sun B and Wang G. Ferroptosis: past, present and future. *Cell Death Dis* 2020; 11: 88.
- [14] Tang D, Chen X, Kang R and Kroemer G. Ferroptosis: molecular mechanisms and health implications. *Cell Res* 2021; 31: 107-125.
- [15] Wang H, Lin D, Yu Q, Li Z, Lenahan C, Dong Y, Wei Q and Shao A. A promising future of ferroptosis in tumor therapy. *Front Cell Dev Biol* 2021; 9: 629150.
- [16] Wang X, Chen Y, Wang X, Tian H, Wang Y, Jin J, Shan Z, Liu Y, Cai Z, Tong X, Luan Y, Tan X, Luan B, Ge X, Ji H, Jiang X and Wang P. Stem cell factor SOX2 confers ferroptosis resistance in lung cancer via upregulation of SLC7A11. *Cancer Res* 2021; 81: 5217-5229.
- [17] Zhang W, Sun Y, Bai L, Zhi L, Yang Y, Zhao Q, Chen C, Qi Y, Gao W, He W, Wang L, Chen D,

## Arsenic trioxide promotes ferroptosis in lung adenocarcinoma stem cells

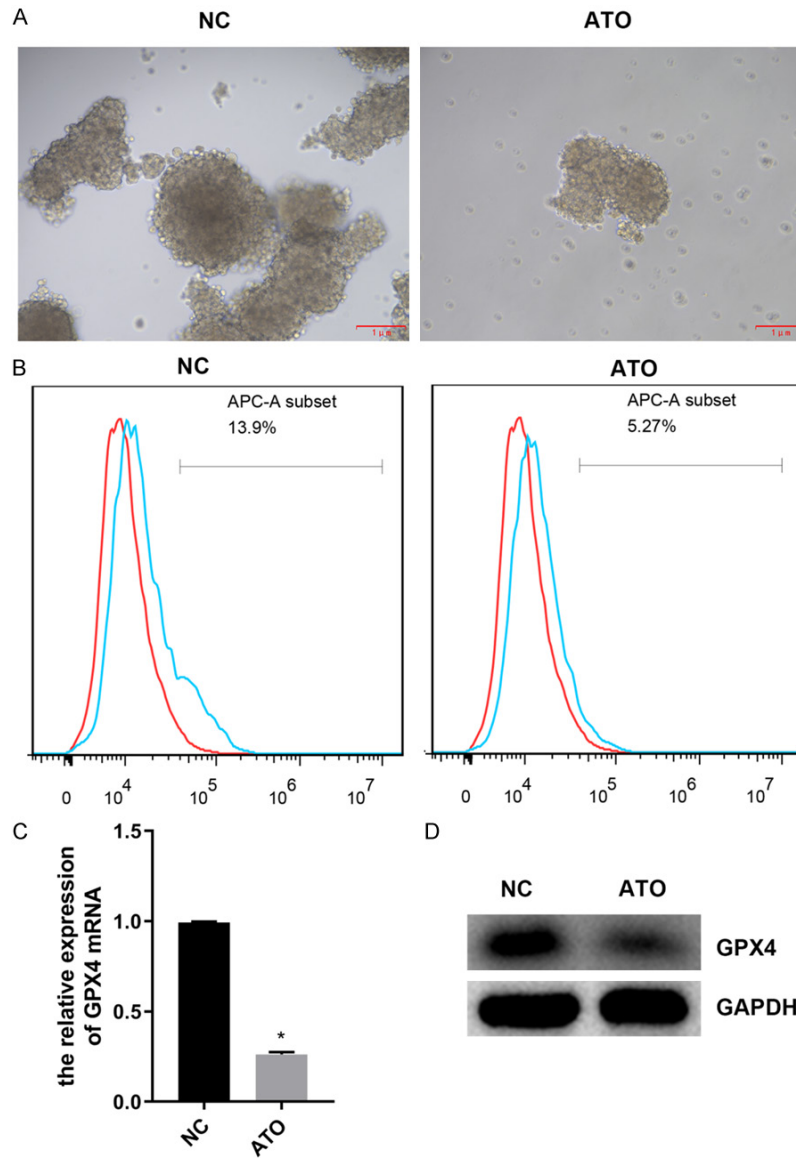
- Fan S, Chen H, Piao HL, Qiao Q, Xu Z, Zhang J, Zhao J, Zhang S, Yin Y, Peng C, Li X, Liu Q, Liu H and Wang Y. RBMS1 regulates lung cancer ferroptosis through translational control of SLC7A11. *J Clin Invest* 2021; 131: e152067.
- [18] Zhang Q, Yi H, Yao H, Lu L, He G, Wu M, Zheng C, Li Y, Chen S, Li L, Yu H, Li G, Tao X, Fu S and Deng X. Artemisinin derivatives inhibit non-small cell lung cancer cells through induction of ROS-dependent apoptosis/ferroptosis. *J Cancer* 2021; 12: 4075-4085.
- [19] Xu Y, Lv D, Yan C, Su H, Zhang X, Shi Y and Ying K. METTL3 promotes lung adenocarcinoma tumor growth and inhibits ferroptosis by stabilizing SLC7A11 m(6)A modification. *Cancer Cell Int* 2022; 22: 11.
- [20] Wang QQ, Hua HY, Naranmandura H and Zhu HH. Balance between the toxicity and anticancer activity of arsenic trioxide in treatment of acute promyelocytic leukemia. *Toxicol Appl Pharmacol* 2020; 409: 115299.
- [21] Sanz MA and Barragan E. History of acute promyelocytic leukemia. *Clin Hematol Int* 2021; 3: 142-152.
- [22] Maiuthed A, Chantawong W and Chanvorachote P. Lung cancer stem cells and cancer stem cell-targeting natural compounds. *Anti-cancer Res* 2018; 38: 3797-3809.
- [23] Leao R, Domingos C, Figueiredo A, Hamilton R, Tabori U and Castelo-Branco P. Cancer stem cells in prostate cancer: implications for targeted therapy. *Urol Int* 2017; 99: 125-136.
- [24] Prabavathy D and Ramadoss N. Heterogeneity of small cell lung cancer stem cells. *Adv Exp Med Biol* 2019; 1139: 41-57.
- [25] Zhang L, Shen L and Wu D. Clinical significance of cancer stem cell markers in lung carcinoma. *Acta Biochim Pol* 2021; 68: 187-191.
- [26] Zhang X, Hu B, Sun YF, Huang XW, Cheng JW, Huang A, Zeng HY, Qiu SJ, Cao Y, Fan J, Zhou J and Yang XR. Arsenic trioxide induces differentiation of cancer stem cells in hepatocellular carcinoma through inhibition of LIF/JAK1/STAT3 and NF- $\kappa$ B signaling pathways synergistically. *Clin Transl Med* 2021; 11: e335.
- [27] Wang HY, Zhang B, Zhou JN, Wang DX, Xu YC, Zeng Q, Jia YL, Xi JF, Nan X, He LJ, Yue W and Pei XT. Arsenic trioxide inhibits liver cancer stem cells and metastasis by targeting SRF/MCM7 complex. *Cell Death Dis* 2019; 10: 453.
- [28] Wu M, Zhang X, Zhang W, Chiou YS, Qian W, Liu X, Zhang M, Yan H, Li S, Li T, Han X, Qian P, Liu S, Pan Y, Lobie PE and Zhu T. Cancer stem cell regulated phenotypic plasticity protects metastasized cancer cells from ferroptosis. *Nat Commun* 2022; 13: 1371.
- [29] Wang Y, Zhao G, Condello S, Huang H, Cardenas H, Tanner EJ, Wei J, Ji Y, Li J, Tan Y, Davuluri RV, Peter ME, Cheng JX and Matei D. Frizzled-7 identifies platinum-tolerant ovarian cancer cells susceptible to ferroptosis. *Cancer Res* 2021; 81: 384-399.
- [30] Xu X, Zhang X, Wei C, Zheng D, Lu X, Yang Y, Luo A, Zhang K, Duan X and Wang Y. Targeting SLC7A11 specifically suppresses the progression of colorectal cancer stem cells via inducing ferroptosis. *Eur J Pharm Sci* 2020; 152: 105450.
- [31] Stockwell BR, Jiang X and Gu W. Emerging mechanisms and disease relevance of ferroptosis. *Trends Cell Biol* 2020; 30: 478-490.
- [32] Seibt TM, Proneth B and Conrad M. Role of GPX4 in ferroptosis and its pharmacological implication. *Free Radic Biol Med* 2019; 133: 144-152.
- [33] Wang T, Kong S, Tao M and Ju S. The potential role of RNA N6-methyladenosine in cancer progression. *Mol Cancer* 2020; 19: 88.
- [34] Jiang X, Liu B, Nie Z, Duan L, Xiong Q, Jin Z, Yang C and Chen Y. The role of m6A modification in the biological functions and diseases. *Signal Transduct Target Ther* 2021; 6: 74.
- [35] Huang H, Weng H and Chen J. m(6)A modification in coding and non-coding RNAs: roles and therapeutic implications in cancer. *Cancer Cell* 2020; 37: 270-288.
- [36] Chen M and Wong CM. The emerging roles of N6-methyladenosine (m6A) deregulation in liver carcinogenesis. *Mol Cancer* 2020; 19: 44.
- [37] Li Y, Sheng H, Ma F, Wu Q, Huang J, Chen Q, Sheng L, Zhu X, Zhu X and Xu M. RNA m(6)A reader YTHDF2 facilitates lung adenocarcinoma cell proliferation and metastasis by targeting the AXIN1/Wnt/ $\beta$ -catenin signaling. *Cell Death Dis* 2021; 12: 479.
- [38] Lin S, Choe J, Du P, Triboulet R and Gregory RI. The m(6)A methyltransferase METTL3 promotes translation in human cancer cells. *Mol Cell* 2016; 62: 335-345.
- [39] Zhang Y, Liu X, Liu L, Li J, Hu Q and Sun R. Expression and prognostic significance of m6A-related genes in lung adenocarcinoma. *Med Sci Monit* 2020; 26: e919644.
- [40] Li Y, Gu J, Xu F, Zhu Q, Chen Y, Ge D and Lu C. Molecular characterization, biological function, tumor microenvironment association and clinical significance of m6A regulators in lung adenocarcinoma. *Brief Bioinform* 2021; 22: bbaa225.

# Arsenic trioxide promotes ferroptosis in lung adenocarcinoma stem cells



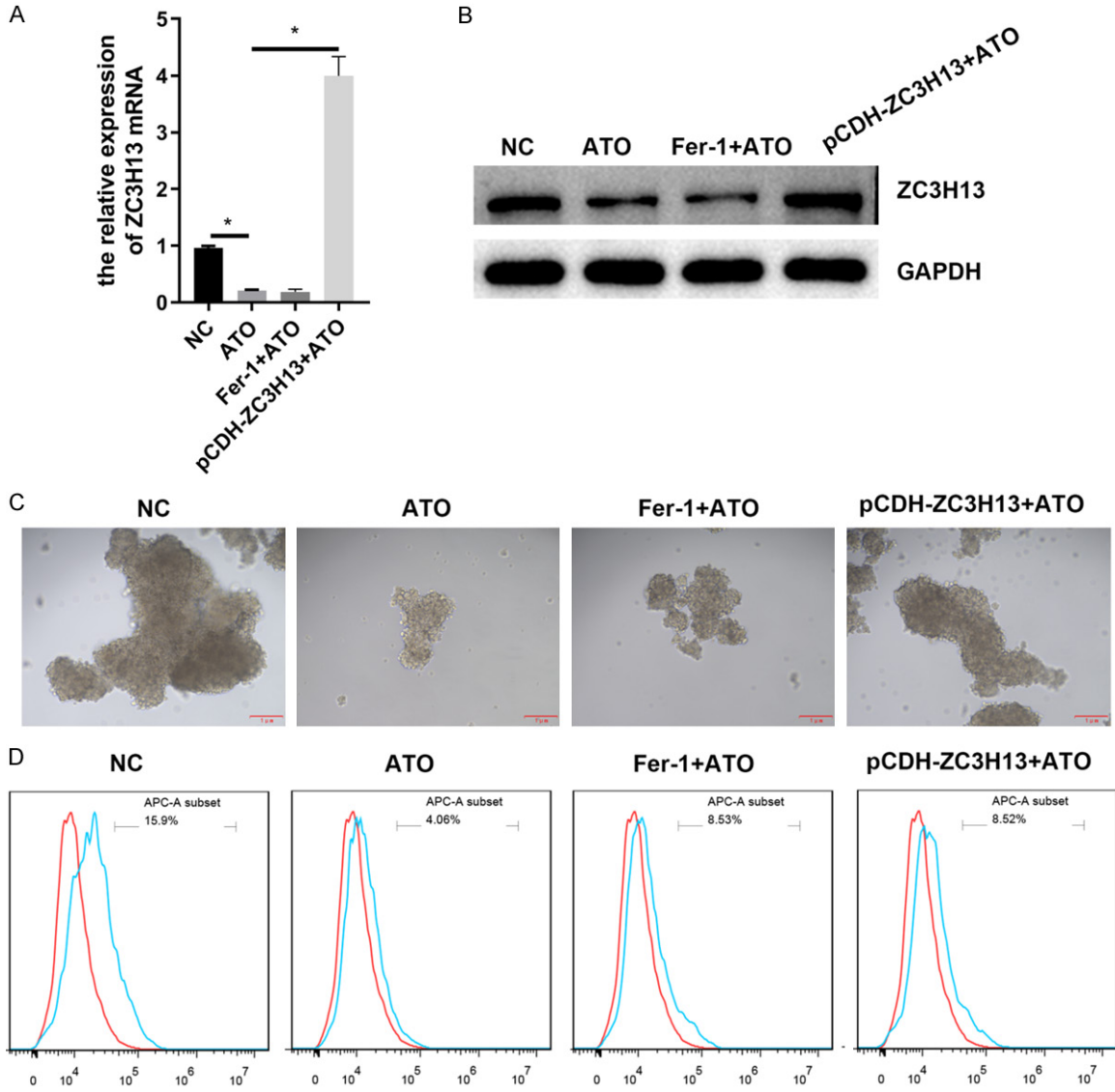
**Supplementary Figure 1.** Inhibition of proliferation and m6A formation by ATO treatment in LASCs from NCI-H1975 cells. (A) Tumorsphere formation in NCI-H1975 cells induced by treatment with the sphere formation medium. Tumor sphere formation after treatment for 1, 3, and 7 days was evaluated using the sphere formation assay. (B) Increase in CD133-positive cells in NCI-H1975 cells treated with sphere formation medium. The percentages of CD133+ cells were measured by flow cytometry. (C) Suppression of LASCs cell viability by ATO treatment for 24 or 48 h. LASCs from NCI-H1975 cells were treated with 0, 0.625, 1.25, 2.5, 5, 10, 20, or 40 mM of ATO, followed by detection of cell viability by the CCK-8 method. (D) Decrease in total m6A content in LASCs from NCI-H1975 cells induced by ATO treatment. The total m6A levels in LASCs from NCI-H1975 cells were determined using the dot blot method. (E and F) Effects of ATO treatment on ZC3H13 expression in LASCs from NCI-H1975 cells. The mRNA (E) and protein (F) levels of ZC3H13 in LASCs were analyzed by quantitative RT-PCR and western blotting, respectively. ATO: arsenic trioxide; LASCs: lung adenocarcinoma stem cells; NC: negative control; ZC3H13: zinc finger CCCH domain-containing protein 13; \*\**P* < 0.01.

# Arsenic trioxide promotes ferroptosis in lung adenocarcinoma stem cells



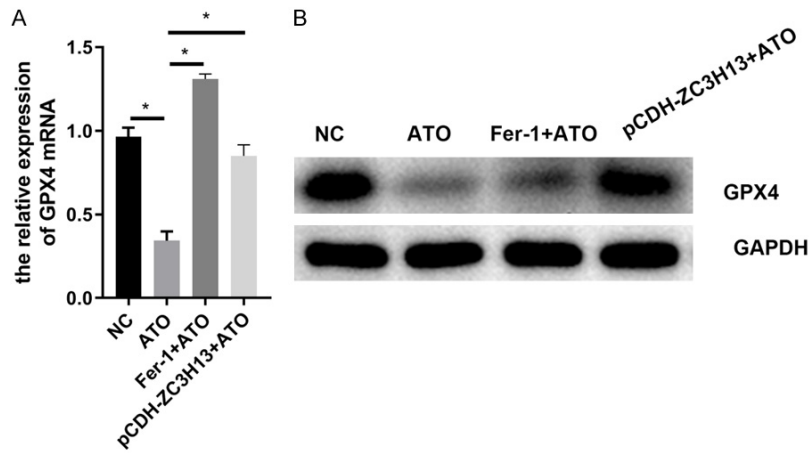
**Supplementary Figure 2.** Modulation of LASCs from NCI-H1975 cells ferroptosis and stemness by ATO treatment. (A) Effects of ATO treatment on the sphere-forming capacities of LASCs. LASCs were treated with 10 mM of ATO for 48 h, and the capacity for tumor sphere formation was evaluated using the tumorsphere formation assay. (B) Decreased percentage of CD133-positive LASCs caused by ATO treatment. The percentages of CD133+ cells were analyzed using the flow cytometry method. (C and D) Inhibition of GPX4 gene expression by ATO treatment in LASCs. The mRNA (C) and protein (D) levels of GPX4 in LASCs were detected by RT-PCR and western blotting, respectively, after treatment with 10 mM of ATO for 24 or 48 h. NC: negative control; ATO: arsenic trioxide; GPX4: glutathione peroxidase 4; GAPDH: glyceraldehyde-3-phosphate dehydrogenase; \* $P < 0.05$ .

Arsenic trioxide promotes ferroptosis in lung adenocarcinoma stem cells

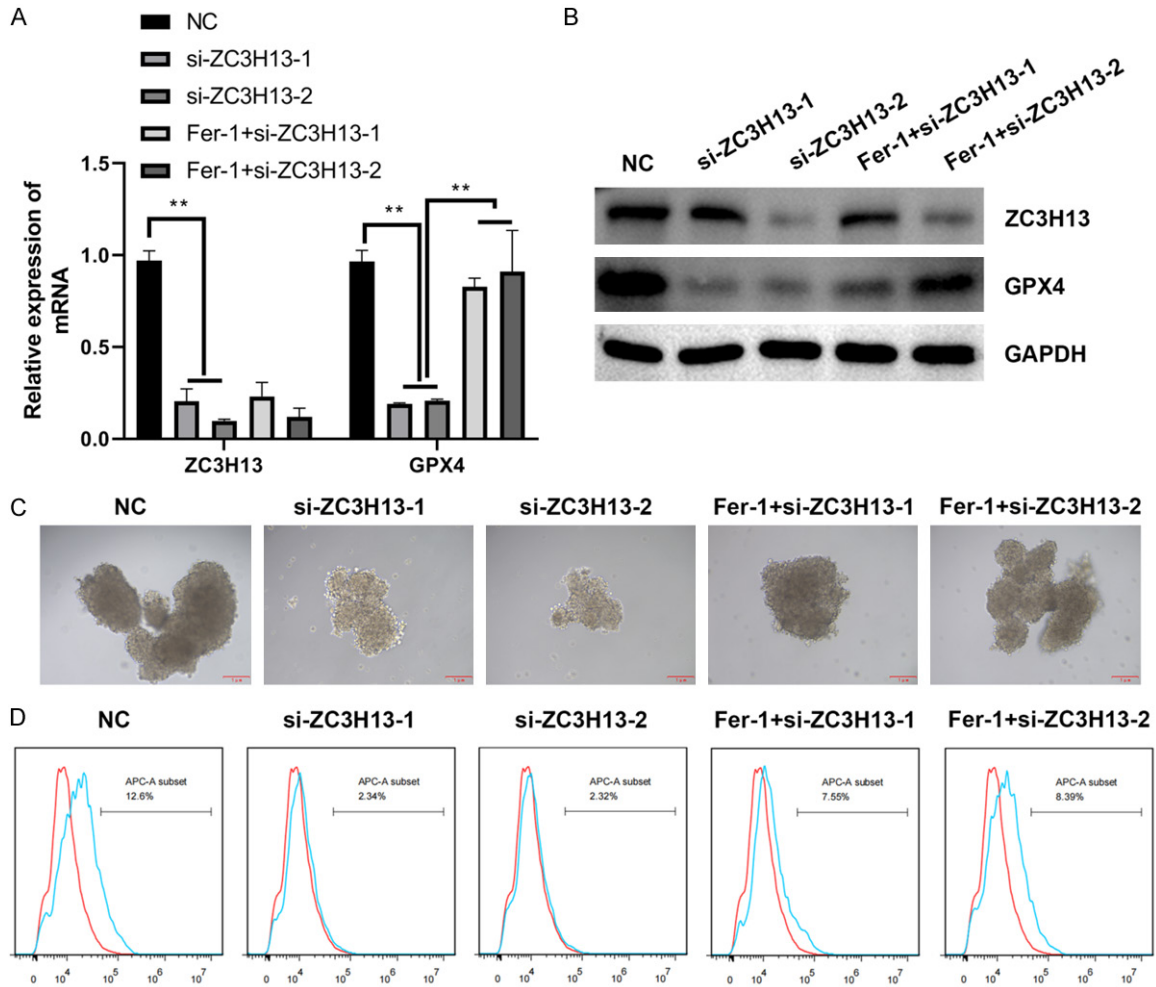


**Supplementary Figure 3.** Effects of ZC3H13 overexpression and Fer-1 on the stemness of LASCs from NCI-H1975 cells. **A.** ZC3H13 mRNA levels in LASCs overexpressing the ZC3H13 gene or treated with Fer-1. ZC3H13 mRNA levels in LASCs were analyzed by quantitative PCR. **B.** ZC3H13 protein abundances in LASCs with ZC3H13 gene overexpression or under the treatment. Western blotting was performed to assess ZC3H13 protein levels. **C.** Promotion of the sphere formation capacity of LASCs under ATO treatment by ZC3H13 overexpression or Fer-1 treatment. The tumorsphere-forming capacity of LASCs was evaluated using the sphere formation assay. **D.** Recovery of the percentages of CD133-positive LASCs under ATO treatment by ZC3H13 gene overexpression or Fer-1 treatment. Percentages of CD133+ LASCs cells were quantitated by flow cytometry. Fer-1: ferrostatin-1; ZC3H13: zinc finger CCCH domain-containing protein 13; NC: negative control; ATO: arsenic trioxide; GAPDH: glyceraldehyde-3-phosphate dehydrogenase; \* $P < 0.05$ .

Arsenic trioxide promotes ferroptosis in lung adenocarcinoma stem cells



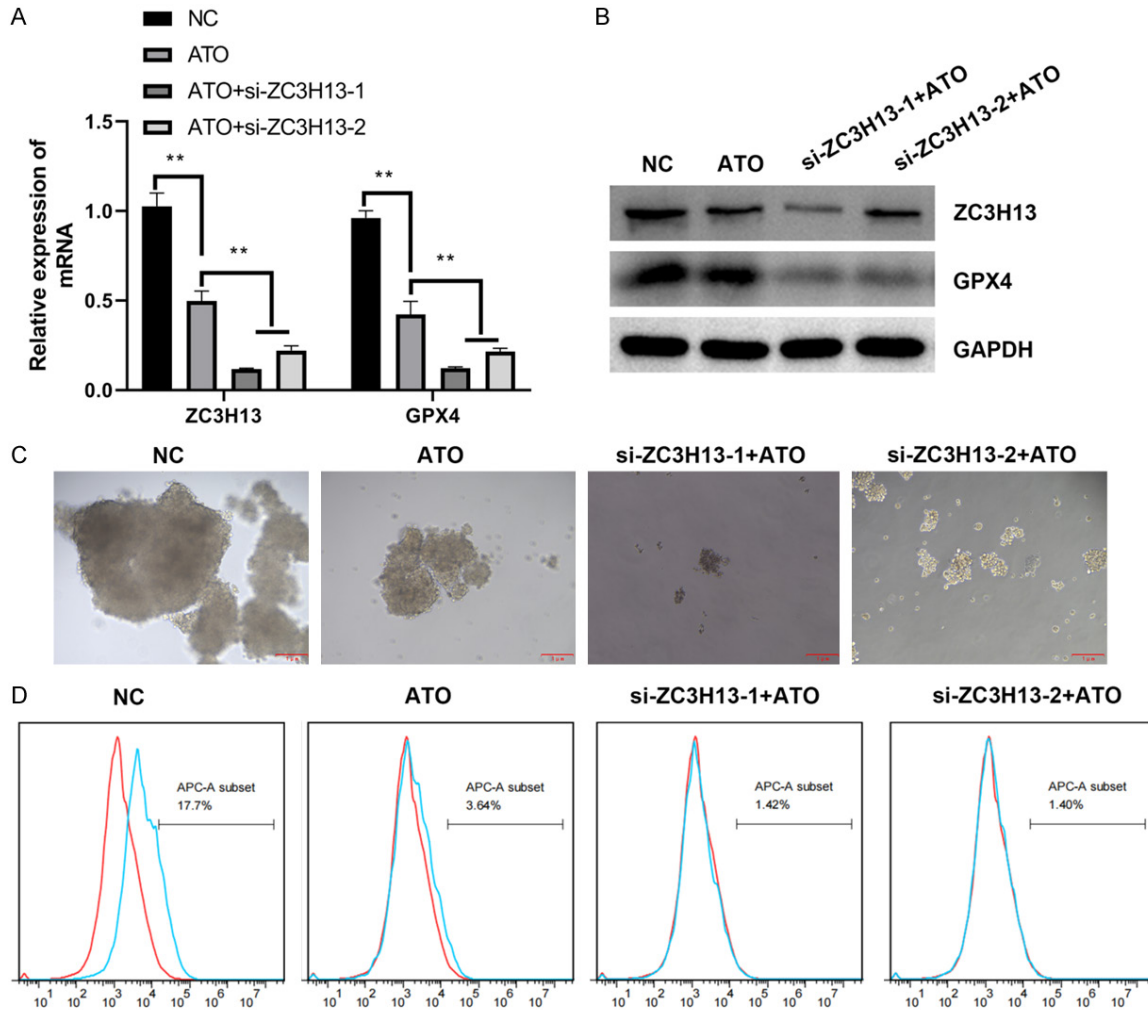
**Supplementary Figure 4.** Elevated GPX4 gene expression in LASCs from NCI-H1975 cells under ATO treatment by Fer-1 treatment or ZC3H13 overexpression. GPX4 mRNA (A) or protein (B) levels in LASCs from NCI-H1975 cells were detected by quantitative PCR and western blotting, respectively.



**Supplementary Figure 5.** Abrogation of si-ZC3H13-induced ferroptosis enhancement and stemness inhibition in LASCs from NCI-H1975 cells by Fer-1 treatment. (A and B) Expression levels of ZC3H13 and GPX4 genes in LASCs treated with si-ZC3H13-1 (or si-ZC3H13-2) and Fer-1. mRNA (A) and protein (B) levels in LASCs were quantitated by quantitative RT-PCR and western blotting, respectively. (C) Recovery of the sphere-forming capacity of ZC3H13-silenced LASCs by Fer-1 treatment. Tumor sphere formation by LASCs was evaluated using the sphere formation

## Arsenic trioxide promotes ferroptosis in lung adenocarcinoma stem cells

assay. (D) Elevation of CD133-positive cell percentages in ZX3H13-silenced LASCs by Fer-1 treatment. Flow cytometry was performed to quantify CD133-positive LASCs percentages. ZC3H13: zinc finger CCCH domain-containing protein 13; NC: negative control; si-ZC3H13-1: siRNA fragment 1 of ZC3H13; si-ZC3H13-2: siRNA fragment 2 of ZC3H13; Fer-1: Ferrostatin-1; GAPDH: glyceraldehyde-3-phosphate dehydrogenase; GPX4: glutathione peroxidase 4; \*\* $P < 0.01$ .



**Supplementary Figure 6.** Effects of interference with ZC3H13 on stemness and ferroptosis in LASCs from NCI-H1975 cells. A. The mRNA levels of ZC3H13 and GPX4 in LASCs interference with ZC3H13 combined with ATO treatment. Quantitative PCR was used to analyze mRNA levels in LASCs. B. Protein abundances of ZC3H13 and GPX4 in LASCs interference with ZC3H13 combined with ATO treatment. Western blot was performed to assess protein levels. C. Promotion of the sphere formation capacity of LASCs interference with ZC3H13 combined with ATO treatment. The tumorsphere-forming capacity of LASCs was assessed by the sphere formation assay. D. Percentages of CD133+ LASCs after ZC3H13 interference combined with ATO treatment. Percentages of CD133+ LASCs cells were quantitated using flow cytometry. ZC3H13: zinc finger CCCH domain-containing protein 13; NC: negative control; si-ZC3H13-1: siRNA fragment 1 of ZC3H13; si-ZC3H13-2: siRNA fragment 2 of ZC3H13; ATO: arsenic trioxide; GAPDH: glyceraldehyde-3-phosphate dehydrogenase; \*\* $P < 0.01$ .